HAL open science

Abscisic acid supports colonization of Eucalyptus grandis roots by the mutualistic ectomycorrhizal fungus Pisolithus microcarpus

Richard Hill, Johanna Wong-Bajracharya, Sidra Anwar, Donovin Coles, Mei Wang, Anna Lipzen, Vivian Ng, Igor Grigoriev, Francis Martin, Ian Anderson, et al.

▶ **To cite this version:**

Richard Hill, Johanna Wong-Bajracharya, Sidra Anwar, Donovin Coles, Mei Wang, et al.. Abscisic acid supports colonization of Eucalyptus grandis roots by the mutualistic ectomycorrhizal fungus Pisolithus microcarpus. New Phytologist, 2022, 233 (2), pp.966-982. ⟨10.1111/nph.17825⟩. ⟨hal-04003919⟩

HAL Id: hal-04003919

https://hal.inrae.fr/hal-04003919v1

Submitted on 24 Feb 2023

HAL is a multi-disciplinary open access archive for the deposit and dissemination of scientific research documents, whether they are published or not. The documents may come from teaching and research institutions in France or abroad, or from public or private research centers.

L'archive ouverte pluridisciplinaire **HAL**, est destinée au dépôt et à la diffusion de documents scientifiques de niveau recherche, publiés ou non, émanant des établissements d'enseignement et de recherche français ou étrangers, des laboratoires publics ou privés.

Distributed under a Creative Commons CC BY 4.0 - Attribution - International License

New Phytologist

Check for updates

Abscisic acid supports colonization of *Eucalyptus grandis* roots by the mutualistic ectomycorrhizal fungus *Pisolithus microcarpus*

Richard A. Hill[1], Johanna Wong-Bajracharya[1,2], Sidra Anwar[1], Donovin Coles[1], Mei Wang[3], Anna Lipzen[3], Vivian Ng[3], Igor V. Grigoriev[3,4], Francis Martin[5], Ian C. Anderson[1], Christopher I. Cazzonelli[1], Thomas Jeffries[6], Krista L. Plett[1,2] and Jonathan M. Plett[1]

[1]Hawkesbury Institute for the Environment, Western Sydney University, Richmond, NSW 2753, Australia; [2]Elizabeth Macarthur Agricultural Institute, New South Wales Department of Primary Industries, Menangle, NSW 2568, Australia; [3]US Department of Energy Joint Genome Institute, Lawrence Berkeley National Laboratory, Berkeley, CA 94720, USA; [4]Department of Plant and Microbial Biology, University of California Berkeley, Berkeley, CA 94720, USA; [5]INRAE, UMR Interactions Arbres/Microorganismes, Laboratory of Excellence ARBRE, INRAE GrandEst-Nancy, Université de Lorraine, 54280 Champenoux, France; [6]School of Science, Western Sydney University, Richmond, NSW 2753, Australia

Author for correspondence:
Jonathan M. Plett
Email: j.plett@westernsydney.edu.au

Received: *26 August 2021*
Accepted: *20 October 2021*

New Phytologist (2022) **233:** 966–982
doi: 10.1111/nph.17825

Key words: carotenoid, ectomycorrhizal fungus, hormone, immunity, plant–microbe interactions, symbiosis.

Summary

- The pathways regulated in ectomycorrhizal (EcM) plant hosts during the establishment of symbiosis are not as well understood when compared to the functional stages of this mutualistic interaction. Our study used the EcM host *Eucalyptus grandis* to elucidate symbiosis-regulated pathways across the three phases of this interaction.
- Using a combination of RNA sequencing and metabolomics we studied both stage-specific and core responses of *E. grandis* during colonization by *Pisolithus microcarpus*. Using exogenous manipulation of the abscisic acid (ABA), we studied the role of this pathway during symbiosis establishment.
- Despite the mutualistic nature of this symbiosis, a large number of disease signalling TIR-NBS-LRR genes were induced. The transcriptional regulation in *E. grandis* was found to be dynamic across colonization with a small core of genes consistently regulated at all stages. Genes associated to the carotenoid/ABA pathway were found within this core and ABA concentrations increased during fungal integration into the root. Supplementation of ABA led to improved accommodation of *P. microcarpus* into *E. grandis* roots.
- The carotenoid pathway is a core response of an EcM host to its symbiont and highlights the need to understand the role of the stress hormone ABA in controlling host–EcM fungal interactions.

Introduction

Eucalyptus grandis, a major forestry crop accounting for > 20 million hectares of timber plantations globally, is known for fast growth and adaptability (Myburg *et al.*, 2014; Wingfield *et al.*, 2015; Vivas *et al.*, 2019). Supporting its growth and establishment, *E. grandis* enters into mutually beneficial symbioses with mycorrhizal fungi including the ectomycorrhizal (EcM) fungus *Pisolithus microcarpus* (Duplessis *et al.*, 2005; Plett *et al.*, 2015a). Mycorrhizal fungi, as a broad class, engage in mutualistic associations with *c.* 93% of all plant species, exchanging mineral nutrients for photosynthetically fixed carbon from the plant. EcM fungi, meanwhile, associate with *c.* 2% of plant species, but their hosts typically make up the dominant flora in most of the forested biomes of the world (Tedersoo *et al.*, 2010; Brundrett & Tedersoo, 2018). As opposed to arbuscular mycorrhizal (AM) fungi, which have specialized fungal hyphae that can penetrate plant cell walls, EcM fungi grow only in the apoplastic space of the root and form a structure called a 'Hartig net' that is the site of the mutualistic exchange of nutrients with the plant (Brundrett & Tedersoo, 2018; Becquer *et al.*, 2019). Given the invasive nature by which EcM fungi colonize their hosts, a number of host transcriptional and metabolic pathways are impacted by these associations, although the pathways that are altered during colonization vary depending on which plant/fungal species are being studied (Larsen *et al.*, 2015; Plett *et al.*, 2015a; Liao *et al.*, 2016; Martin *et al.*, 2016; Bouffaud *et al.*, 2020).

Regardless of type, all mycorrhizal fungi follow the same three general stages of root colonization: an initial stage of pre-symbiosis prior to physical interaction during which signals are exchanged between the two organisms, a stage of physical integration during which the fungus aggregates on the root surface and then begins to grow into the root followed by a final stage of functional symbiosis during which the fungus is established within the root and nutrients begin to be exchanged between the two partners (Hogekamp & Küster, 2013; Plett *et al.*, 2015b). The progression through each of these stages is thought to involve both a distinct set of differentially regulated genes that

© 2021 The Authors
New Phytologist © 2021 New Phytologist Foundation. This article has been contributed to by US Government employees and their work is in the public domain in the USA.

14698137, 2022, 2, Downloaded from https://nph.onlinelibrary.wiley.com/doi/10.1111/nph.17825 by Inrae - Dipso, Wiley Online Library on [24/02/2023]. See the Terms and Conditions (https://onlinelibrary.wiley.com/terms-and-conditions) on Wiley Online Library for rules of use; OA articles are governed by the applicable Creative Commons License

14698137, 2022, 2, Downloaded from https://nph.onlinelibrary.wiley.com/doi/10.1111/nph.17825 by Inrae - Dipso, Wiley Online Library on [24/02/2023]. See the Terms and Conditions (https://onlinelibrary.wiley.com/terms-and-conditions) on Wiley Online Library for rules of use; OA articles are governed by the applicable Creative Commons License

support the stage-specific metabolic and physical changes taking place, as well as persistent set of genes whose change in expression are required to enable the symbiotic interaction (Hogekamp & Küster, 2013; Garcia *et al.*, 2015; Larsen *et al.*, 2015; Plett *et al.*, 2015b).

During the pre-symbiotic stage, EcM fungi secrete a cocktail of signalling molecules, including proteins and other soluble and volatile metabolites (Menotta *et al.*, 2004a,b; Splivallo *et al.*, 2009; Garcia *et al.*, 2015; Cope *et al.*, 2019; Wong *et al.*, 2019; Rush *et al.*, 2020; Plett *et al.*, 2021a). Upon perception of these signals, physical and metabolic changes occur within the plant, underpinned by a change in gene expression (Sebastiana *et al.*, 2009; da Silva Coelho *et al.*, 2010; Li *et al.*, 2014; Larsen *et al.*, 2015; Wong *et al.*, 2019). Metabolites induced within the host during the early stages of colonization include flavonoids, fatty acids, terpenoids, and carotenoids (Wong *et al.*, 2019). Genes involved in the plant immune system are typically repressed (Seddas *et al.*, 2009; Garcia *et al.*, 2015; Wong *et al.*, 2019). Lateral root formation is also stimulated by EcM fungal signals independent of contact (Felten *et al.*, 2009; Splivallo *et al.*, 2009; Ditengou *et al.*, 2015). Contact and integration between the two organisms trigger further metabolic and physical changes in the host. During this stage of the interaction, plant transcriptomic changes linked to pathways involved with immune and stress responses have been reported, as have increases in gene expression of signal receptors (Sebastiana *et al.*, 2009; Balestrini & Bonfante, 2014; Larsen *et al.*, 2015; Plett *et al.*, 2015b; Liao *et al.*, 2016). In the final stage of the interaction, during which the fungus becomes fully established within the host as determined by the presence of a Hartig net, plant nutrient transporter genes are induced and nutrient fluxes between the partner organisms can be measured (Duplessis *et al.*, 2005; Willmann *et al.*, 2014; Garcia *et al.*, 2015; Hortal *et al.*, 2017; Basso *et al.*, 2019; Plett *et al.*, 2020; Plett *et al.*, 2021b).

Many phytohormones are important to the development of EcM interactions, with previous research highlighting how the sensitivity to, and regulation of, plant hormones such as jasmonic acid, ethylene, and auxin affect colonization (Plett *et al.*, 2014; Basso *et al.*, 2019). In addition to these classic phytohormones, only a few studies in EcM fungi have explored the role of abscisic acid (ABA) in host interactions (Luo *et al.*, 2009; Calvo-Polanco *et al.*, 2019; Lorente *et al.*, 2021) despite the finding of its crucial role in the establishment of AM fungal symbioses (Herrera-Medina *et al.*, 2007; Charpentier *et al.*, 2014; Lou *et al.*, 2021). ABA is synthesized from carotenoids and functions to coordinate the plant's response to abiotic stress as well as promote pathogen defence responses (Finkelstein, 2013; Jia *et al.*, 2017; Fiorilli *et al.*, 2019). Carotenoids can also be cleaved into other apocarotenoid metabolites important for plant–microbe interactions, such as strigolactones and blumenin which have been found to be significant to establishment of AM symbiosis (Maier *et al.*, 1995; Akiyama *et al.*, 2005; Besserer *et al.*, 2006; Stauder *et al.*, 2018). Carotenoids can also serve to reduce damage from stress-induced oxidation in some plant–mycorrhizal interactions (Alvarez *et al.*, 2009; Hamilton & Bauerle, 2012).

In this study we sought to further our understanding of the *E. grandis* genomic pathways that are significantly regulated during the colonization process of the EcM fungus *P. microcarpus*. Using transcriptional profiling across the major stages of EcM root colonization, we present significantly regulated host signalling pathways associated with specific interaction phases. The carotenoid biosynthetic pathway and ABA signalling processes were highly enriched with significantly altered gene expression throughout this interaction, thereby representing a core response of *E. grandis* to *P. microcarpus* colonization. We quantified ABA during the fungal integration steps pathway and found that the synthesis of ABA is significantly regulated by the presence of *P. microcarpus*. Exogenous application of ABA altered Hartig net development of *P. microcarpus,* suggesting that ABA may play a more important role in EcM symbiosis than previously found.

Materials and Methods

Plant and fungal growth conditions and mycorrhizal root tip formation

Eucalyptus grandis seeds (Seed lot 20 974) were obtained from the Commonwealth Scientific and Industrial Research Organization tree seed centre (CSIRO, Clayton, Australia). *Pisolithus microcarpus* isolate SI-14 was isolated from a single fruiting body from Sussex Inlet (36°50 041″S, 150°59 086″E), New South Wales, Australia (scientific license number S13146). *Eucalyptus grandis* seeds were sterilized in 30% hydrogen peroxide (H_2O_2, v/v) for 10 min and then washed with sterile deionized water five times prior to germination on 1% (w/v) water agar and incubated in a controlled environment growth cabinet for one month (25°C; 16 h light cycle). Following this, seedlings were transferred into half-strength modified Melin–Norkrans (MMN) media (pH 5.5; 1 g l^{-1} glucose; 1% agar) placed between two cellophane membranes to prevent growth into the media (Kleerview Covers by Fowlers Vacola Manufacturing Co. Ltd, Melbourne, VIC, Australia) and grown for another month (22–30°C night/day temperature; 16 h light cycle). Two weeks before contact with the plants, *P. microcarpus* SI-14 was propagated onto cellophane covered half-strength MMN plates and grown in the dark at 25°C. All Petri dishes used were Sarstedt 92 × 16 mm polystyrene vented plates.

Once the *E. grandis* seedlings were two months old and the fungal cultures were 2 wk old, the plants were separated into one of three treatment categories: (1) 'axenic controls' consisted of seedlings transferred onto new half-strength MMN medium without any fungal inoculum; (2) 'pre-symbiosis seedlings' were transferred onto new half-strength MMN medium in indirect contact with fungal mycelium for 24 h by separating the two organisms by a permeable cellophane membrane; (3) 'physical contact' seedlings were transferred onto new half-strength MMN medium and then placed into direct contact with the active growing edge of a fungal colony and then samples were harvested at 24 h, 48 h, 1 wk, and 2 wk post-contact. These plates were then closed using micropore tape to allow for gas exchange with the external environment.

© 2021 The Authors
New Phytologist © 2021 New Phytologist Foundation. This article has been contributed to by US Government employees and their work is in the public domain in the USA.

14698137, 2022, 2, Downloaded from https://nph.onlinelibrary.wiley.com/doi/10.1111/nph.17825 by Inrae - Dipso, Wiley Online Library on [24/02/2023]. See the Terms and Conditions (https://onlinelibrary.wiley.com/terms-and-conditions) on Wiley Online Library for rules of use; OA articles are governed by the applicable Creative Commons License

RNA extraction, sequencing, and analysis

The plant root tips of each group were harvested and immediately frozen in liquid nitrogen. For each timepoint, three biological replicates were harvested and extracted. Root samples were then stored in a −80°C freezer until RNA extraction. The RNA from each of the samples was then extracted using the ISOLATE II Plant miRNA kit (Bioline, Sydney, Australia) as per the manufacturer's instructions. Following extraction, the RNA samples were sequenced at the Joint Genome Institute (JGI). Plate-based RNA sample preparation was performed using the Perkin Elmer Sciclone NGS robotic liquid handling system, utilizing Illumina's TruSeq Stranded mRNA HT sample prep kit utilizing poly-A selection of messenger RNA (mRNA) following the protocol outlined by Illumina in their user guide for TruSeq Stranded mRNA workflow: https://support.illumina.com/sequencing/sequencing_kits/truseq-stranded-mrna-workflow.html with the following conditions: total RNA starting material was 100 ng per sample and 10 cycles of PCR was used for library amplification.

The prepared RNA-sequencing (RNA-Seq) libraries were then quantified using KAPA Biosystem's next-generation sequencing library qPCR kit, run on a Roche LightCycler 480 real-time PCR instrument. Quantified RNA-Seq libraries were then multiplexed with other libraries. This pool of libraries was then prepared for sequencing on the Illumina HiSeq sequencing platform, utilizing a TruSeq paired-end cluster kit (v4) and Illumina's cBot instrument to generate a clustered flow cell for sequencing. Sequencing of the flow cell was then performed on the Illumina HiSeq2500 sequencer using HiSeq TruSeq SBS sequencing kits (v4), following a 2 × 150 indexed run recipe. The JGI QC pipeline was then used to filter and trim the raw RNA-Seq reads. These raw RNA-Seq reads were then evaluated for artefact sequence by kmer matching (kmer = 25), allowing one mismatch and detected artefact, trimmed from the 3′ end of the reads using BBDuk (https://sourceforge.net/projects/bbmap/). Following this, RNA spike-in reads, PhiX reads and reads containing any Ns were removed. Quality trimming was then performed using the Phred trimming method, set at Q6. Following trimming, reads under the minimum length threshold of 25 bases were removed unless one-third of the original read length of those reads were longer. The filtered reads from each RNA-Seq library were then all aligned with the *E. grandis* genome, identifying each gene sequence and their existing characterization (Myburg *et al.*, 2014). This characterization includes their gene ontology (GO), KEGG (Kyoto Encyclopedia of Genes and Genomes) identifier (ID) and closest *Arabidopsis thaliana* homologue. Only primary hits assigned to the reverse strand were included in the raw gene counts (-s 2 -p −−primary options). The gene count data was used to identify significantly differentially expressed genes (DEGs) using DEseq2 v.1.30.0 in Rstudio v.4.0.3 (Love *et al.*, 2014). Relative $\log_2$-fold change was calculated through pairwise comparison of each timepoint to axenic plant-only controls using DEseq2. These values were then sorted by significance whereby a DEG was deemed to have a $\log_2$-fold change of greater than 1 and a *P*-value (adjusted for false-discovery; P_{adj}) of ≤ 0.05. Normalized, rlog transformed count data was used to perform principal component analysis (PCA) using the MixOmics package v.6.14.0 in Rstudio. The Pearson statistical method was used to calculate the relative similarity dendrogram, using all 6687 genes to measure the relative similarity of each timepoint based on their differential gene expression profiles. Heat-map figures were produced using Morpheus (https://software.broadinstitute.org/morpheus).

The RNA-Seq expression patterns were validated using quantitative polymerase chain reaction (qPCR). Briefly, RNA from these root tips was used to synthesize complementary DNA (cDNA) using the Tetro cDNA synthesis kit (Bioline) according to manufacturer's instructions using only the oligo dT_{18} primer and a standardized quantity of RNA. The qPCR reaction utilized SensiFAST SYBR no-ROX Q-PCR kit (Bioline) following manufacturers' instructions. The expression levels of two plant control genes (*Eucgr.C00350* and *Eucgr.K02046*) were used to normalize the results and the $\log_2$-fold change was calculated for 12 genes across all timepoints (Supporting Information Table S1). These expression values were plotted against the $\log_2$-fold change of each gene using a bivariate scatter plot. The significance of the correlation was determined.

Gene enrichment and KEGG analyses

Gene enrichment analyses were used to identify which genomic pathways were significantly overrepresented within the data. These were performed using two different programs to improve the robustness of the analyses. PlantRegMap (Tian *et al.*, 2020; http://plantregmap.gao-lab.org) was used with *E. grandis* gene IDs for GO enrichment while gProfiler utilized the orthologous *A. thaliana* gene ID as a complementary enrichment tool and were both performed at $P < 0.05$ (Raudvere *et al.*, 2019). In order to further investigate genes and metabolic pathways regulated during the different colonization timepoints considered, we utilized the KEGG mapper tool (https://www.genome.jp/kegg/; accessed 8 March 2020) to associate the *E. grandis* DEGs to known metabolic pathways using the KEGG orthology (KO) numbers associated with each gene within the data set (Kanehisa & Goto, 2000; Kanehisa *et al.*, 2017, 2019). Heat maps were generated and overlaid onto the carotenoid metabolic pathways of interest to show the relative differential gene expression over time using the Morpheus online tool. The carotenoid pathway utilized in this article was based on Sandmann (2021).

Carotenoid analysis

Using the same conditions as described earlier, we generated *E. grandis* seedlings in pre-symbiotic contact with *P. microcarpus* SI-14 for 48 h or their complementary axenic controls, after which the roots were harvested and immediately frozen in liquid nitrogen and stored at −80°C. Root samples from *c.* 10 individual plants were pooled to obtain a recommended minimum of 150 mg of tissue for each replicate for total carotenoid extraction. A total of four independent replicates were extracted per group. A pre-symbiotic setup was chosen as we could sample root-only tissue, thereby avoiding the quantification of potential

© 2021 The Authors
New Phytologist © 2021 New Phytologist Foundation. This article has been contributed to by US Government employees and their work is in the public domain in the USA.

14698137, 2022, 2, Downloaded from https://nph.onlinelibrary.wiley.com/doi/10.1111/nph.17825 by Inrae - Dipso, Wiley Online Library on [24/02/2023]. See the Terms and Conditions (https://onlinelibrary.wiley.com/terms-and-conditions) on Wiley Online Library for rules of use; OA articles are governed by the applicable Creative Commons License

carotenoids that may be also produced by the fungus. Frozen roots were finely ground using a mortar and pestle containing liquid nitrogen and extracted in 500 µl of extraction buffer (acetone : ethyl acetate; 60 : 40 v/v) containing 0.1% BHT (butylated hydroxytoluene). An equal volume of MilliQ water was then added to each tube, gently inverted to avoid forming an emulsion and centrifuged for 5 min at 15 000 ***g***. The upper phase was transferred to a glass vial and pigments separated via high-performance liquid chromatography (HPLC) using a C18 column. Absolute quantification of xanthophyll pigments was performed as previously described in Cazzonelli *et al.* (2020) and Alagoz *et al.* (2020).

Abscisic acid responsive genes

ABA responsive genes were identified and classed based on *A. thaliana* genomic annotation, and cross-checked with the *E. grandis* annotation where available, as well as previously published literature (Amir Hossain *et al.*, 2010; Kulik *et al.*, 2011; Finkelstein, 2013). Genes involved in ABA metabolism and transport, signalling and/or regulated by ABA in *E. grandis* were also annotated against those identified in *A. thaliana* as previously described by Pornsiriwong *et al.* (2017). These ABA responsive genes were then extracted from our relative gene expression matrices and analysed for significant differential expression as described earlier. The expression of various classes of ABA responsive genes were then visualized in heat map form through the MORPHEUS platform.

Abscisic acid quantification

Eucalyptus grandis plants and fungi were grown in the same way as for the time course analysis focusing on the pre-symbiotic timepoint and the fungal integration timepoints (24 h post-contact through 1 wk). At a given timepoint, roots in contact with fungi, or in indirect contact with fungal colonies for pre-symbiosis, were excised from the surrounding mycelium and pooled to obtain 30–40 mg of tissue per replicate. Four separate replicates for plant tissues were extracted as detailed later. To understand if ABA was being produced in *P. microcarpus* mycelium in close contact to the roots, we also excised from the plates fungal mycelium that had been physically touching the root system. As with the roots, samples were pooled to obtain 30–40 mg of tissue per replicate. Due to the small masses recovered, we obtained three separate replicates for these tissues per timepoint. ABA was extracted according to the method of Hall *et al.* (2019) with modifications. In brief, *c.* 50 mg ground root tissue per sample was extracted with 70% methanol spiked with 2H-ABA (Olchemim, Olomouc, Czech Republic) to yield a final 2H-ABA concentration of 100 ppb. All samples were incubated in a rotor mixer at 80 rpm for 30 min at 4°C before centrifuging at 16 000 ***g*** for 5 min at room temperature. The supernatant was then collected into a clean tube and the samples re-extracted with 70% methanol to reach a final volume of 250 µl. The extracts were analysed by ultra-performance liquid chromatography electrospray ionization tandem mass spectrometry (UPLC-ESI-MS/MS) using an Acquity UHPLC coupled to a Xevo triple quadrupole mass spectrometer (Waters Corp., Milford, CT, USA). Briefly, 5 µl of extract were injected into a 2.1 mm × 50 mm × 1.7 µm, C18 reverse phase column. ABA identification was based on comparison to fragmentation pattern with an authentic standard. Quantification was based on a standard calibration curve and adjusted for sample recovery as compared to the internal ABA standard. Reported ABA values within the manuscript were either fold-change from ABA concentrations in axenic tissues or as absolute concentrations with standard error.

The effect of exogenous abscisic acid on colonization

In order to ascertain the effect of exogenous ABA application upon symbiosis, the *E. grandis–P. microcarpus* interaction was repeated as described earlier for the 'physical contact' condition but with the addition of ABA to the media in the interaction plates. The concentrations chosen were 0, 0.1, 0.25, and 0.5 µM of ABA ($n = 6$). ABA was dissolved in ethanol and added to the medium after autoclaving. Dilutions were done such that an equivalent amount of ethanol was added to all treatments (including 0 µM). To verify that the added hormones were not affecting the pH of the medium, we tested this and found that pH was not affected by the addition of ABA (Fig. S1). After a 2-wk period of colonization, the total number of root tips exhibiting a fungal mantle were counted as opposed to the number of uncolonized roots in contact with the fungus. Normalcy of the colonized and uncolonized root data was assayed using a Shapiro–Wilk test and the significance of the data analysed using a Student's *t*-test. Roots exhibiting mantle formation were excised from the plants and fixed in 4% paraformaldehyde and stored at 4°C until sectioning. To section, samples were embedded in 6% agarose and 30 µm thick cross-sections were cut using a 7000SMZ-2 Vibrotome (Campden Instrument Ltd, London, UK) and stored in 1 × phosphate-buffered saline (PBS, pH 7.4) at 4°C until staining. The roots were each sectioned in the middle of the colonized root tip to ensure the most comparable results. Roots were rinsed three times with 1 × PBS (pH 7.4) after co-staining with Wheat Germ Agglutinin-Fluorescein (WGA-FITC; 100 µg ml^{-1}) for 15 min and propidium iodide (PI; 20 µg ml^{-1}) for 10 min. Confocal microscopy was carried out on a TCS SP5 confocal laser scanning microscope (Leica, Macquarie Park, NSW, Australia) with an excitation wavelength of 488 nm and detection wavelength of 500–550 nm for WGA-FITC imaging and a 561 DPSS laser with an excitation wavelength of 561 nm and detection wavelength of 580–660 nm for PI staining. Plant/fungal contact area was calculated using measurements of sections of each root imaged. Each image was imported into IMAGEJ and the contact surface area of fungal hyphae to plant cells was measured using the free-hand tool and normalized to the outer circumference of the root. Six biological replicates were measured per condition, with two technical replicates per biological replicate. Hartig net depth of penetration and mantle thickness were also measured using IMAGEJ. The former measurement is defined as the distance from the outer rim of a

© 2021 The Authors
New Phytologist © 2021 New Phytologist Foundation. This article has been contributed to by US Government employees and their work is in the public domain in the USA.

given epidermal cell to the deepest point of fungal penetration. An average of five technical replicate measurements for each root section image were taken and then averaged to arrive at a value for each biological replicate. Similarly, mantle thickness was a measurement from the outer rim of epidermal cells to the outer rim of the fungal mantle.

To quantify the relative fungal biomass within each colonized root, and support the results obtained from microscopic analysis, we undertook a qPCR approach. This approach was taken as relative mantle thickness was found to be consistent between treatments suggesting that any difference in fungal biomass would be due to increased fungal presence within the root. Individual colonized root tips from four biological replicates of *E. grandis* treated with either 0.25 µM ABA or control were excised from the root systems ensuring that no excess extra-radical mycelium was taken. cDNA was synthesized as earlier. The expression level of two fungal control genes (*Pm_670570,* and *Pm_679335*; i.e. known to show consistent expression regardless of conditions) and one plant control gene (*Eucgr. C00350*) were assayed using the SensiFAST SYBR no-ROX Q-PCR kit (Bioline) following the manufacturers' instructions. To quantify the copy number of each gene, we PCR amplified each of the target sequences, purified them using the Wizard SV Gel and PCR Clean-Up system (Promega, Madison, WI, USA) according to the manufacturer's instructions and generated a standard curve with known numbers of copies to relate transcript copy number to Ct in our qPCR cycling. Following this, the average ratio of fungal gene expression : plant gene expression was calculated.

Results

Host gene expression shows the greatest variation during the integration stage of *P. microcarpus* colonization

Colonization of the *E. grandis* root system by the mutualistic fungus *P. microcarpus* isolate SI-14 led to 6687 significant plant DEG ($P < 0.05$; Table S2) across five timepoints of colonization, ranging from pre-symbiosis through to a fully colonized mycorrhizal root tip at 2 wk post-contact (Fig. 1a). These data were further verified using qPCR (Fig. S1a). There was a significant correlation between the transcriptional profile predicted by RNA-Seq and gene transcription based on qPCR analysis ($R^2 = 0.31$, $r = 0.56$; $F(1,52) = 23.27$; $P < 0.001$; $\beta = 0.91$; $P < 0.001$). We found that the lowest number of DEGs was observed during the pre-symbiotic phase, when the plant and fungus were separated physically by a permeable membrane, followed by the 2 wk timepoint. This latter timepoint shows a fully developed Hartig net, the development of which has previously been demonstrated to lead to active exchange of nutrients with the host plant in similar *in vitro* conditions (Hortal *et al.*, 2017; Plett *et al.*, 2020). Between these two timepoints are those timepoints concerning the physical integration stage of colonization, covering the timepoints 24 h post-contact through to the 1-wk timepoint, where we observed the majority of DEGs. Additionally, we observed that there were nearly equal numbers of genes that were upregulated or downregulated (Fig. 1a). A comparison of DEGs from each of the three stages of colonization indicated that a relatively small number of genes were found to be persistently regulated throughout colonization, the majority of which were significantly upregulated (106 that were persistently upregulated throughout colonization, one gene that was upregulated in certain stages and repressed in others, three genes were persistently repressed; Fig. 1b). The 109 persistently regulated gene set made up nearly half of the DEGs during the pre-symbiotic timepoint, whilst also being the third largest grouping in the 2-wk functional symbiosis timepoint.

Hierarchical clustering of the samples based on expression patterns showed clustering of the timepoints during the physical integration stages apart from the pre-symbiotic and functional symbiotic timepoints (Fig. 1c). In order to identify the genes most responsible for driving differences between the timepoints we performed a PCA with our time course data. We found that principal component one (PC1) explained 31.5% of the variation, followed by 14.3% for principal component two (PC2) (Fig. 1d). Therefore, as PC1 presented the same distribution of groupings observed in the dendrogram, we identified those genes having the largest contribution to this PC. These genes most explain the separation of the timepoints during which the fungus is integrating into the root from the pre-symbiotic or the functional (i.e. 2 wk) timepoints. Within this gene set, 13 genes had a percentage contribution of > 0.25 and were significantly differentially regulated across the time course of colonization (Fig. 1e; Table S3). All but one of the 13 influential DEGs were primarily upregulated throughout colonization with the top three genes being an ABA-induced protein phosphatase gene (PP2C; Eucgr.A01486), a *LATE EMBRYOGENESIS ABUNDANT* gene (Eucgr.K01836), and a *Eucalyptus*-specific gene of unknown function (Eucgr.H04961; Fig. 1e). The repressed gene was annotated as a polyketide cyclase/dehydrase and lipid transport superfamily protein (Eucgr.L02071; Fig. 1e). Separation of colonization timepoints along PC2 was largely driven by nutrient and lipid transporters (Table S4).

Eucalyptus grandis root metabolism changes over the course of *P. microcarpus* colonization

The metabolic pathways regulated in *E. grandis* over the course of colonization were identified using annotated GO terms within our datasets (Table 1). During the integration stages, genes associated with the flavonoid and phenylpropanoid biosynthesis pathways were significantly repressed while the latter became positively regulated during functional symbiosis at 2 wk post-contact. Beyond KEGG pathway enrichment, we also considered the enriched biological processes at each of the timepoints and found that genes involved in defence or response to abiotic stress were typically upregulated during the integration stages of colonization (i.e. 24 h and 48 h post-contact timepoints through 1 wk post-contact) after which they were repressed at 2 wk (Table 1). There was also enrichment of genes associated with two main hormone pathways: the ABA response and degradation pathway (GO:0010295; GO:0009737) as well as auxin response and transport (GO:0080161; 35 auxin responsive DEGs, associated and transport related genes).

© 2021 The Authors
New Phytologist © 2021 New Phytologist Foundation. This article has been contributed to by US Government employees and their work is in the public domain in the USA.

14698137, 2022, 2, Downloaded from https://nph.onlinelibrary.wiley.com/doi/10.1111/nph.17825 by Inrae - Dipso, Wiley Online Library on [24/02/2023]. See the Terms and Conditions (https://onlinelibrary.wiley.com/terms-and-conditions) on Wiley Online Library for rules of use; OA articles are governed by the applicable Creative Commons License

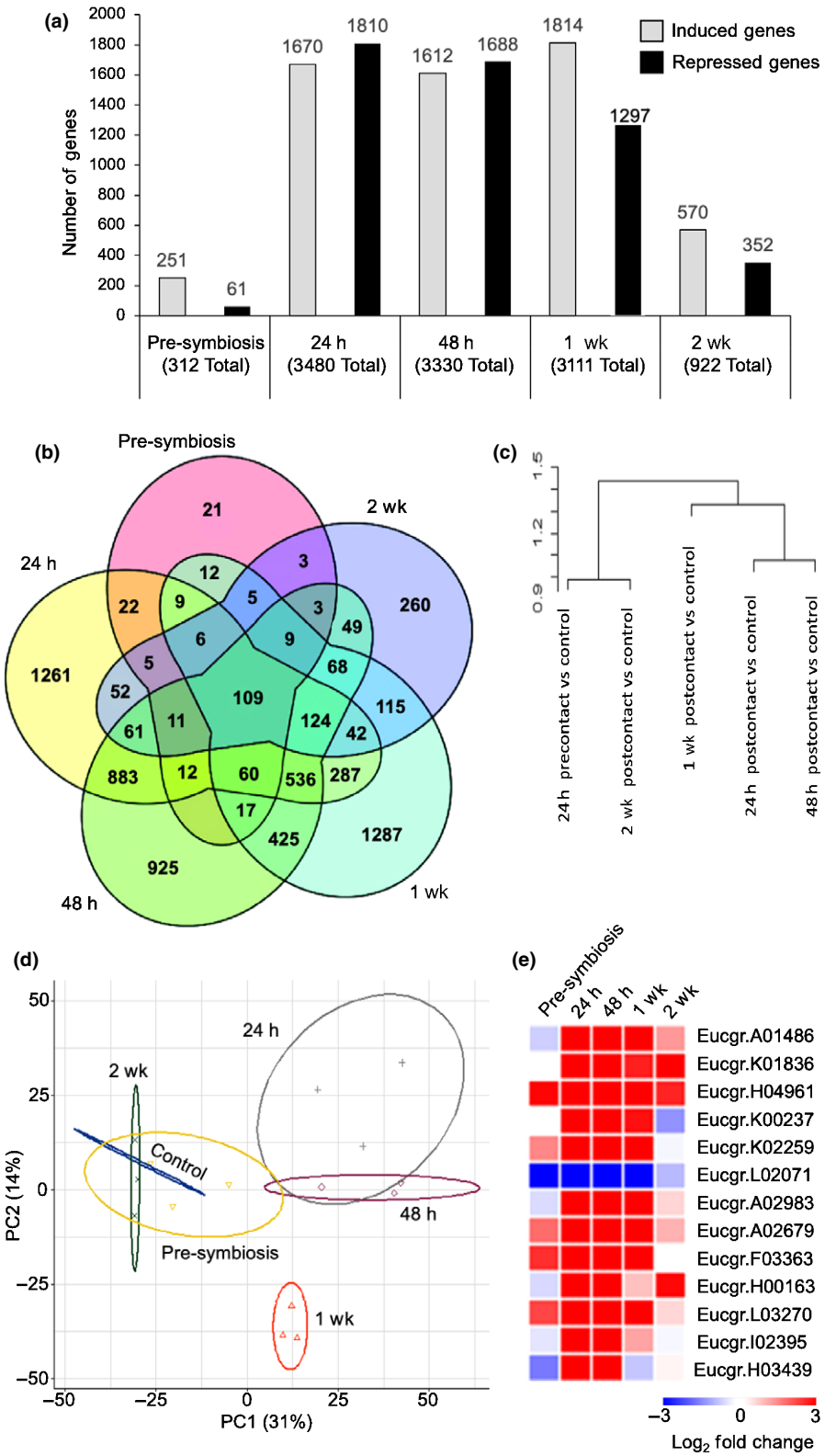

Fig. 1 Altered transcription of different pathways in *Eucalyptus grandis* linked to each stage of colonization by *Pisolithus microcarpus*. (a) Bar graph showing the number of significant positively and negatively expressed genes at each timepoint (grey bars and black bars, respectively; $P < 0.05$). (b) Venn diagram showing the number of common differentially expressed genes (DEGs) between all five timepoints and all genes unique to individual timepoints. Total number of DEGs within each category are shown. (c) Dendrogram demonstrating the relative similarity of each timepoint based on DEG profiles. (d) Principal component analysis of normalized and r-log transformed transcriptomic data for each replicate across the time course of colonization. (e) Heatmap showing the relative expression of genes most responsible for the separation of the timepoints during *P. microcarpus* colonization of *E. grandis* along the principal component one (PC1) axis with a percentage contribution to PC1 > 0.25.

Finally, we considered the enriched processes associated with the 109 persistently DEGs (Table 2). Genes associated with terpenoid and tetraterpenoid metabolism, lipid metabolism, as well as monocarboxylic acid biosynthesis were found to be abundant.

Based on the consistent enrichment of defence and stress response genes we extracted those genes contributing to the enriched GO defence term, annotated as TIR-NBS-LRR gene family, NB-ARC domain-containing resistance proteins, and dirigent-like protein family. Of the 234 genes across these classes,

© 2021 The Authors
New Phytologist © 2021 New Phytologist Foundation. This article has been contributed to by US Government employees and their work is in the public domain in the USA.

14698137, 2022, 2, Downloaded from https://nph.onlinelibrary.wiley.com/doi/10.1111/nph.17825 by Inrae - Dipso, Wiley Online Library on [24/02/2023]. See the Terms and Conditions (https://onlinelibrary.wiley.com/terms-and-conditions) on Wiley Online Library for rules of use; OA articles are governed by the applicable Creative Commons License

Table 1 Significantly enriched processes associated with root function during the colonization of *Eucalyptus grandis* by *Pisolithus microcarpus*.

Timepoint	Expression relative to axenically grown roots	Number of significantly regulated genes ($P < 0.05$)	Enriched GO terms KEGG (gProfiler; $P < 0.05$)	Enriched GO biological processes (PlantRegMap; $P < 0.01$)
Pre-symbiosis (24 h indirect contact)	Positive	251	N/A	ADP binding Defence response Carotenoid metabolism Phenylpropanoid processes
	Negative	61	N/A	Cellulose synthase Glucosyltransferase ADP binding
24 h (post-contact)	Positive	1670	MAPK signalling pathway Tyrosine metabolism Carotenoid biosynthesis Biosynthesis of secondary metabolites	Response to abiotic stress Transcription factor activity Transporters Response to abscisic acid (ABA) Response to hormone Carotenoid biosynthesis
	Negative	1810	Metabolic pathways DNA replication Biosynthesis of secondary metabolites Flavonoid biosynthesis Nitrogen metabolism	Catalytic activity DNA replication Response to abiotic stress
48 h (post-contact)	Positive	1612	Protein processing in endoplasmic reticulum Galactose metabolism	Response to abiotic stress Response to ABA Voltage-gated ion channel activity
	Negative	1688	Phenylpropanoid biosynthesis Metabolic pathways Biosynthesis of secondary metabolites Glyoxylate and dicarboxylate metabolism Zeatin biosynthesis	Response to abiotic stress Oxidoreductase activity Cell wall biosynthesis
1 wk (post-contact)	Positive	1814	N/A	ADP binding Ribonucleotide binding Nucleotide binding Response to stress Defence response Signal transduction
	Negative	1217	Ribosome	Plastid
2 wk (post-contact)	Positive	570	Phenylpropanoid biosynthesis	Oxidoreductase activity Phenylpropanoid biosynthesis Nutrient reservoir activity Extracellular region and cell membrane
	Negative	352	Porphyrin metabolism Metabolic pathways Biosynthesis of secondary metabolites Carbon fixation	Oxidoreductase activity Response to abiotic stress Carotenoid biosynthesis Plastid

Selected enriched KEGG pathways (gProfiler; $P < 0.05$) and gene ontology (GO) biological processes (PlantRegMap; $P < 0.05$) identified amongst the significantly regulated *E. grandis* genes. N/A indicates that no significantly enriched terms were found in this category.

163 were significantly differentially regulated in at least one timepoint (Fig. 2). The TIR-NBS-LRR and NB-ARC domain-containing genes were mostly upregulated across the time course while the dirigent-like proteins were nearly all downregulated.

Genes involved in carotenoid biosynthesis were significantly enriched and differentially regulated throughout colonization

We investigated if there were overrepresented metabolic pathways differentially expressed throughout the whole of the colonization process. For this analysis, we looked for KEGG metabolic pathway gene enrichment within all 6687 DEGs. Of the overrepresented metabolic pathways related to root biology, we found that carotenoid and zeatin biosynthesis pathways exhibited a mixture of both positive and negative gene expression patterns while the phenylpropanoid biosynthesis pathway, metabolism of glyoxylate and dicarboxylate compounds, and flavonoid biosynthesis were universally repressed (Fig. 3a). Fig. 3(b) shows that overrepresented genes pertaining to cellular components were most commonly associated with the cellular membrane and plastid components.

Given the persistence of different carotenoid genes throughout all our analyses, and the fact that plastid related functions were

© 2021 The Authors
New Phytologist © 2021 New Phytologist Foundation. This article has been contributed to by US Government employees and their work is in the public domain in the USA.

14698137, 2022, 2, Downloaded from https://nph.onlinelibrary.wiley.com/doi/10.1111/nph.17825 by Inrae - Dipso, Wiley Online Library on [24/02/2023]. See the Terms and Conditions (https://onlinelibrary.wiley.com/terms-and-conditions) on Wiley Online Library for rules of use; OA articles are governed by the applicable Creative Commons License

14698137, 2022, 2, Downloaded from https://nph.onlinelibrary.wiley.com/doi/10.1111/nph.17825 by Inrae - Dipso, Wiley Online Library on [24/02/2023]. See the Terms and Conditions (https://onlinelibrary.wiley.com/terms-and-conditions) on Wiley Online Library for rules of use; OA articles are governed by the applicable Creative Commons License

Table 2 Enrichment analysis of biological processes from the 109 significant, persistently differentially expressed genes (DEGs) during *Pisolithus microcarpus* colonization of *Eucalyptus grandis*.

Gene ontology (GO) identifier (ID)	GO term	Total number of annotated genes in genome	Number of genes within our DEG dataset	Number of genes expected in a random sample
GO:0006952	Defence response	1028	11	3.14
GO:0043531	ADP binding	791	10	2.57
GO:0016119	Carotene metabolic process	10	2	0.03
GO:0045735	Nutrient reservoir activity	113	4	0.37
GO:0030145	Manganese ion binding	114	4	0.37
GO:0005576	Extracellular region	583	7	1.54
GO:0008610	Lipid biosynthetic process	359	6	1.1
GO:0042214	Terpene metabolic process	19	2	0.06
GO:0016109	Tetraterpenoid biosynthetic process	23	2	0.07
GO:0016117	Carotenoid biosynthetic process	23	2	0.07
GO:0044255	Cellular lipid metabolic process	469	6	1.43
GO:0006950	Response to stress	2325	15	7.09
GO:0072330	Monocarboxylic acid biosynthetic process	203	4	0.62
GO:0016108	Tetraterpenoid metabolic process	31	2	0.09
GO:0016116	Carotenoid metabolic process	31	2	0.09
GO:0006629	Lipid metabolic process	700	7	2.14
GO:0016469	Proton-transporting two-sector ATPase complex	57	2	0.15

Results based on output using the gene enrichment tool PlantRegMap ($P < 0.01$; Tian *et al.*, 2020).

also enriched, we further investigated the expression of the carotenoid pathway as a whole. From this analysis, *E. grandis* homologues to the carotenoid biosynthesis enzymes from *Arabidopsis* were identified and their expression mapped onto the carotenoid biosynthesis pathway (Fig. 4a). The first committed step in carotenoid biosynthesis involves the production of phytoene that, via a series of desaturations and isomerizations is converted into lycopene, that then diverges into the production of epsilon- and beta-carotenoids and downstream xanthophylls. This first step is controlled by PHYTOENE SYNTHASE (PSY; Fig. 4a); of the three genes encoded by *E. grandis,* one gene was significantly downregulated (Eucgr.F02914; *c.* four-fold; Table S5) during the pre-symbiotic phase followed by a steady loss of this repression throughout the physical integration timepoints (i.e. 24 h, 48 h and 1-wk post-inoculation). Commensurate with the earliest timepoint, we found that during pre-symbiosis in between *E. grandis* roots and *P. microcarpus* a reduction in carotenoid concentration in the host tissues was observed (Table 3). Following this stage, genes encoding the following steps of the synthesis of lycopene were generally induced. This was most significantly and strongly seen for *ZETA-CAROTENE DESATURASE* (*ZDS*), which were significantly regulated across all points of colonization ($P < 0.05$; Fig. 4a; Table S5) and represent the carotenoid annotated genes found within the 109 core gene set of *E. grandis'* response to *P. microcarpus* (Fig. 1b). Following this, the biosynthetic pathway branches into the formation of strigolactones and apocarotenoids, β-carotenoids, and lutein. Genes coding for enzymes towards the lutein (*CYP97A/C*) and strigolactone pathways (*CCD7/8*) were not significantly regulated during the early timepoints of the colonization process (Fig. 4a; Table S5). Transcription of genes encoding enzymes responsible for apocarotenoid synthesis (*CCD1/4*) were much more variable in expression across colonization, but the only gene showing significant expression (Eucgr.D02555) was repressed > four-fold during fungal integration into the roots ($P < 0.05$). Conversely, we found a significant induction of β-CAROTENE 3-HYDROZYLASE (BCH; Fig. 4a) during the integration stages of fungal colonization as well as the following steps involving *ZEAXANTHIN EPOXIDASE* (ZEP; Fig. 4a; Table S5; $P < 0.05$). This latter observation was coupled with a significant reduction in the expression of *VIOLAXANTHIN DE-EPOXIDASE* (VDE; Eucgr.B02180; Fig. 4a; $P < 0.05$) which encodes the enzyme which reverses the flux in metabolism at this point of the pathway. The step of neoxanthin to xanthoxin governed by 9-CIS-EPOXYCAROTENOID DIOXYGENASE (NCED; Fig. 4a) also exhibited genes that were universally significantly induced by the colonization process ($P < 0.05$). Taken together, the majority of gene expression profiles in this pathway would suggesting a flux towards biosynthesis of ABA in the later stages of this pathway.

Abscisic acid biosynthesis and responsive genes are altered by symbiosis

In addition to highlighting the carotenoid pathway, enrichment analysis of the biological processes GO terms in Table 1 revealed a large number of genes in the early stages of physical interaction between *P. microcarpus* and *E. grandis* were associated with ABA signalling responses, an apocarotenoid compound and plant hormone. As our transcriptomic results may suggest an increased degradation of the xanthophyll precursors via increased *NCED* expression leading to ABA synthesis during the integration of the fungus into the root apoplastic space, we quantified ABA in roots of *E. grandis* during pre-symbiosis through to the latter stage of fungal integration into the root (i.e. 1 wk). In comparison to axenically grown roots, we found that ABA concentrations

© 2021 The Authors
New Phytologist © 2021 New Phytologist Foundation. This article has been contributed to by US Government employees and their work is in the public domain in the USA.

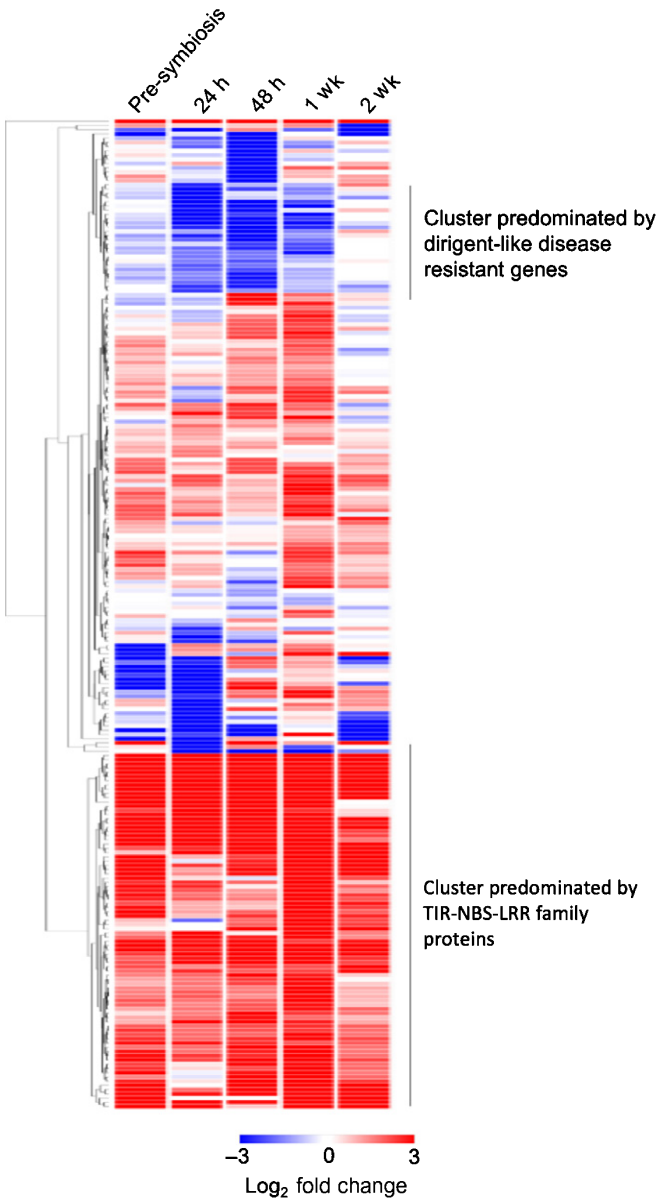

Fig. 2 *Eucalyptus grandis* NBS-LRR genes are induced across colonization by *Pisolithus microcarpus*. Heatmap showing the relative expression of 234 defence related genes within the NB-ARC, NBS-LRR, and dirigent-like classes during *P. microcarpus* colonization of *E. grandis*.

increased > 50× after 24 h of contact with the fungus, an induction that fell to between 9- and 16-fold induction at the later timepoints (Fig. 4b). The increase in ABA concentrations was significant at all timepoints with the exception of pre-symbiosis (Table 4), but was found to be highest at 24 and 48 h post-contact with the fungus. As these tissues are a hybrid between plant and fungus, we also analysed the concentration of ABA in extramatrical mycelium (EMM) adjacent to the root as an estimate of fungal contribution to ABA synthesis. We found that ABA concentrations in comparison to axenically grown fungal cultures mildly increased during pre-symbiosis and then fell to approximately half the original concentration by 48 h post-contact (Fig. 4c), although at no timepoint were the differences in concentrations found to be significantly different from axenic controls (Table 4). Across the samples taken, plant tissues had up to 400× higher concentrations of ABA than the EMM (Table 4).

In order to gauge the transcriptional alterations of ABA-associated genes, we profiled the expression of genes known to be either ABA-induced (Fig. 4d) or ABA-repressed (Fig. 4e) across the time course of colonization based on gene classifications by Pornsiriwong *et al.* (2017). We found a total of 72 *E. grandis* genes orthologous to *A. thaliana* genes known to be induced by ABA, 45 of which were found to be significantly differentially regulated in *E. grandis* during colonization (Fig. 4d). This gene set includes the PP2C genes Eucgr.G02960, Eucgr.J02003 and Eucgr.A01486, the latter of which is included in the gene set most significantly separating the integration stages of our transcriptomic time course from pre-symbiosis and functional symbiosis (Fig. 1e). Of the 75 *E. grandis* genes orthologous to *A. thaliana* ABA-repressed genes, 35 were found to be differentially regulated (Fig. 4e).

Exogenous abscisic acid increases Hartig net development of *P. microcarpus*

Owing to the ABA responsive gene analysis and ABA accumulation during fungal integration into the root, we tested the effect of exogenous ABA upon colonization to see if this would alter colonization potential of *P. microcarpus*. In all treatments we found that *E. grandis* was able to form mycorrhizal roots with the formation of Hartig nets (Fig. 5a–d). The absolute number of colonized roots per plant was not significantly impacted (Fig. 5e). Despite a trend towards increased lateral rooting when the seedlings were grown on higher levels of ABA, we did not observe a significant increase in the number of observed lateral roots ($P = 0.07$). Similarly, mantle formation was unaffected by the ABA treatments (Fig. 5f). Therefore, exogenous ABA does not appear to improve the formation of mantle-encased roots during the colonization of *E. grandis*. Since ABA responsive genes were most frequently induced during the physical integration stage of colonization, and as the concentration of ABA within the roots was highest during the earliest stages of colonization, we reasoned that Hartig net development may have been affected. Based on measurements of Hartig net penetration depth into the root apoplastic space, we found that Hartig net formation was significantly promoted when the plant was treated with exogenous levels of ABA ≥ 0.25 μM (Fig. 5g). We also observed that, in addition to the fungus penetrate deeper into the root system, epidermal plant cells were more elongated and that the fungus appeared to be in greater contact with cortical cells at higher concentrations of ABA (Fig. 5d). Therefore, we measured the difference in fungal contact with root cell between the treatments (i.e. the amount of direct contact between fungal hyphae and plant cells in a transverse cross-section of a colonized root normalized to root circumference). We found that exogenous application of ABA significantly increased the contact area between the fungus and plant cells at all ABA treatments (Fig. 5h). We further wished to verify if increased contact area resulted in a greater fungal biomass within the root tissues. As mantle thickness was not

© 2021 The Authors
New Phytologist © 2021 New Phytologist Foundation. This article has been contributed to by US Government employees and their work is in the public domain in the USA.

14698137, 2022, 2, Downloaded from https://nph.onlinelibrary.wiley.com/doi/10.1111/nph.17825 by Inrae - Dipso, Wiley Online Library on [24/02/2023]. See the Terms and Conditions (https://onlinelibrary.wiley.com/terms-and-conditions) on Wiley Online Library for rules of use; OA articles are governed by the applicable Creative Commons License

14698137, 2022, 2, Downloaded from https://nph.onlinelibrary.wiley.com/doi/10.1111/nph.17825 by Inrae - Dipso, Wiley Online Library on [24/02/2023]. See the Terms and Conditions (https://onlinelibrary.wiley.com/terms-and-conditions) on Wiley Online Library for rules of use; OA articles are governed by the applicable Creative Commons License

(a)

KEGG		stats	
Term name	Term ...	P_{adj}	$-\log_{10}(P_{adj})$ (0 – ≤16)
Biosynthesis of secondary metabolites	KEGG:01110	1.254×10^{-5}	
Metabolic pathways	KEGG:01100	1.112×10^{-4}	
Carotenoid biosynthesis	KEGG:00906	5.289×10^{-4}	
Phenylpropanoid biosynthesis	KEGG:00940	4.537×10^{-3}	
Zeatin biosynthesis	KEGG:00908	1.140×10^{-2}	
Glyoxylate and dicarboxylate metabolism	KEGG:00630	2.088×10^{-2}	
Flavonoid biosynthesis	KEGG:00941	3.947×10^{-2}	

Expression pattern: Over-expression | Mixed expression | Repressed

(b)

GO:CC		stats	
Term name	Term ...	P_{adj}	$-\log_{10}(P_{adj})$ (0 – ≤16)
Cell periphery	GO:0071944	3.429×10^{-25}	
Cell part	GO:0044464	4.060×10^{-18}	
Cell	GO:0005623	6.972×10^{-18}	
Plasma membrane	GO:0005886	6.536×10^{-17}	
Thylakoid	GO:0009579	1.458×10^{-14}	
Plastid thylakoid	GO:0031976	6.647×10^{-14}	
Apoplast	GO:0048046	1.256×10^{-13}	
Plastid thylakoid membrane	GO:0055035	2.080×10^{-13}	
Plastid part	GO:0044435	1.321×10^{-12}	
Organelle subcompartment	GO:0031984	7.749×10^{-11}	
Plastid	GO:0009536	1.091×10^{-8}	
Cell-cell junction	GO:0005911	8.828×10^{-8}	
Cell junction	GO:0030054	8.828×10^{-8}	
Plasmodesma	GO:0009506	8.828×10^{-8}	
Symplast	GO:0055044	9.752×10^{-8}	
External encapsulating structure	GO:0030312	1.125×10^{-7}	
Cell wall	GO:0005618	1.542×10^{-7}	
Plastid envelope	GO:0009526	3.291×10^{-7}	

Expression pattern: Over-expression | Mixed expression | Repressed

Fig. 3 Carotenoid biosynthesis genes are significantly overrepresented within the core transcriptomic response of *Eucalyptus grandis* roots during colonization by *Pisolithus microcarpus*. (a) *Eucalyptus grandis* root-associated metabolic pathways significantly enriched during *P. microcarpus* colonization of *E. grandis* ($P < 0.05$). (b) Gene ontology enrichment analysis of root-associated cellular component pathways in *E. grandis* during *P. microcarpus* colonization ($P < 0.05$).

significantly affected (Fig. 5f), we undertook a qPCR based approach to quantify the ratio between the transcription of stably expressed fungal genes vs stably expressed plant genes. We found that the addition of ABA led to a significantly higher ratio of fungal transcripts vs plant transcripts at the ABA concentration tested (64.4% ± 16% increase), further supporting the results of ABA supporting fungal growth within roots (Fig. 5i). As pH of the medium was unaffected by the addition of ABA (Fig. S1b), and as equivalent amounts of solvent were added to each medium, it is unlikely that the difference in phenotype was due to these factors. Therefore, ABA appears to be involved in the accommodation of *P. microcarpus* into the apoplastic space of *E. grandis* roots.

Discussion

The accommodation of a fungal symbiont within root tissues requires the coordination of a large number of plant metabolic and developmental pathways (Martin *et al.*, 2016). Along with morphological changes, differential host gene expression has been previously linked to the stage of colonization in other model EcM interactions (Duplessis *et al.*, 2005; Le Quéré *et al.*, 2005; Sebastiana *et al.*, 2014; Bouffaud *et al.*, 2020). In this article, we have identified how gene expression changes over time within *E. grandis* roots undergoing *P. microcarpus* colonization. Within our current dataset, the pre-symbiotic and functional stages exhibited the least amount of DEGs as compared to axenic roots, while

© 2021 The Authors
New Phytologist © 2021 New Phytologist Foundation. This article has been contributed to by US Government employees and their work is in the public domain in the USA.

each of the timepoints during fungal integration showed a high number of unique DEGs. This is likely due to the fact that at the final timepoint, the fungus is no longer actively invading the root and the plant is largely restricted to nutrient exchange, thus necessitating fewer regulated pathways. The difference between pre-symbiosis and 24 h post-contact is likely due to the addition of nonsecreted proteins of the fungus (e.g. cell wall proteins) coming into contact with key receptors on the plant host that activate a number of microbe sensitive pathways. Investigating those biological processes most significantly enriched found that

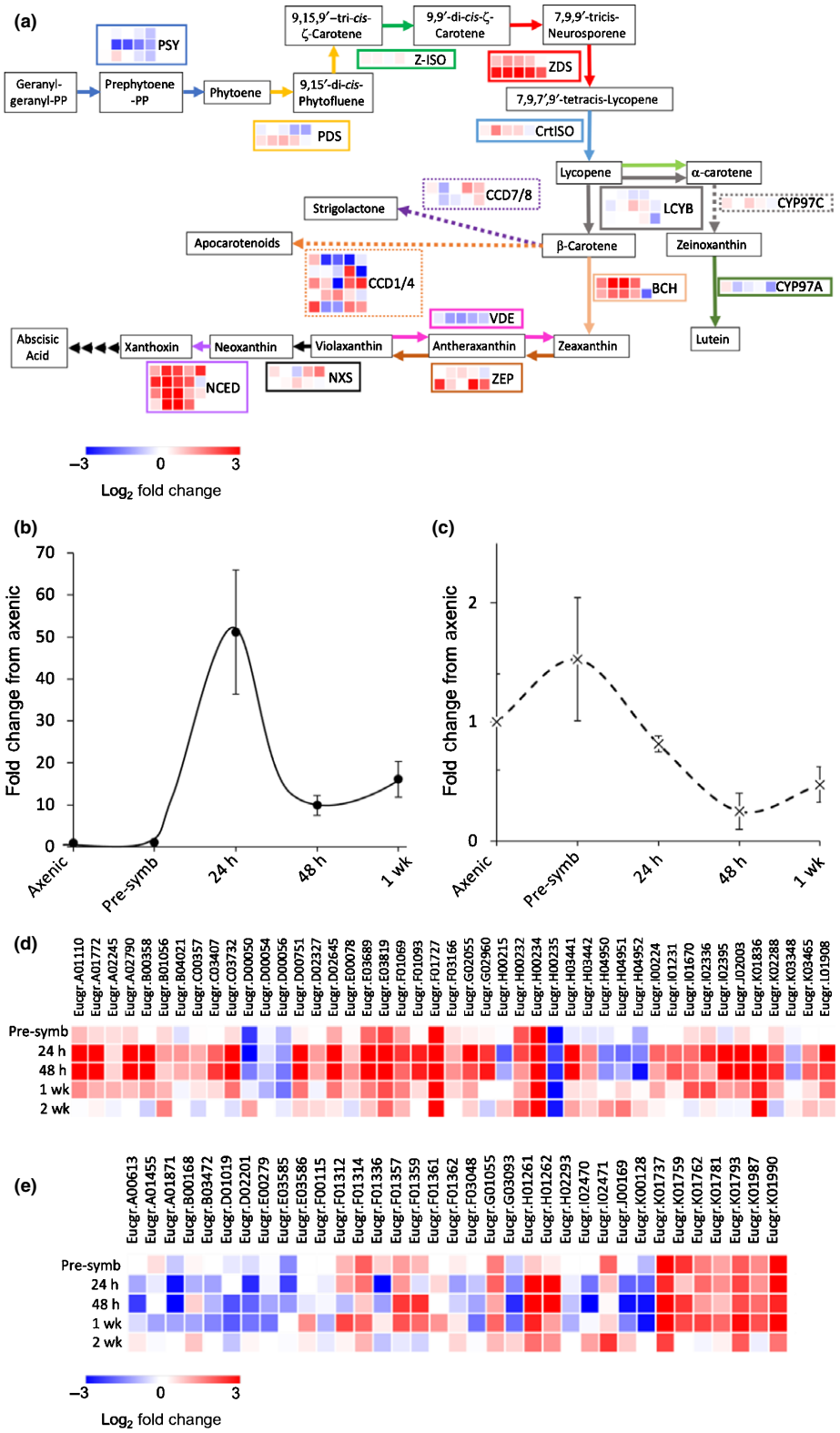

© 2021 The Authors
New Phytologist © 2021 New Phytologist Foundation. This article has been contributed to by US Government employees and their work is in the public domain in the USA.

14698137, 2022, 2, Downloaded from https://nph.onlinelibrary.wiley.com/doi/10.1111/nph.17825 by Inrae - Dipso, Wiley Online Library on [24/02/2023]. See the Terms and Conditions (https://onlinelibrary.wiley.com/terms-and-conditions) on Wiley Online Library for rules of use; OA articles are governed by the applicable Creative Commons License

14698137, 2022, 2, Downloaded from https://nph.onlinelibrary.wiley.com/doi/10.1111/nph.17825 by Inrae - Dipso, Wiley Online Library on [24/02/2023]. See the Terms and Conditions (https://onlinelibrary.wiley.com/terms-and-conditions) on Wiley Online Library for rules of use; OA articles are governed by the applicable Creative Commons License

Fig. 4 Abscisic acid (ABA) concentration increases and ABA responsive genes are significantly regulated during *Pisolithus microcarpus* colonization of *Eucalyptus grandis*. (a) *Eucalyptus grandis* carotenoid biosynthetic pathway with accompanying heatmaps showing $\log_2$-fold change in the expression of genes encoding key enzymes in the pathway. The colour and dash style of the arrows link to the same colour/dash style of boxes around each heatmap serve to match the expression of each enzyme-encoding gene to their specific metabolic step. For each enzyme-encoding gene, five timepoints of expression are presented corresponding to pre-symbiosis followed by 24 h, 48 h, 1 wk, and 2 wk post-contact, respectively, from left to right. Pathway map adapted from the KEGG carotenoid biosynthesis reference pathway (Kanehisa & Goto, 2000; Kanehisa *et al*., 2017, 2019) and all enzymes are labelled with their gene abbreviation as follows: PSY, phytoene synthase; PDS, 15-cis-phytoene desaturase; Z-ISO, ζ-carotene isomerase; ZDS, ζ-carotene desaturase; CrtISO, prolycopene isomerase; LCYE, lycopene epsilon-cyclase; LCYB, lycopene beta-cyclase; BCH, β-carotene 3-hydroxylase; CYP97A/C, carotenoid epsilon hydroxylase A/C; CCD1/4/7/8, carotenoid cleavage diosygenase; ZEP, zeaxanthin epoxidase; VDE, violaxanthin de-epoxidase; NXS, neoxanthin synthase; NCED, 9-*cis*-epoxycarotenoid dioxygenase. Fold change expression values with annotation of significance vs axenically grown *E. grandis* roots can be found in Supporting Information Table S5. (b) Fold change in the concentration of ABA in *E. grandis* roots, as compared to axenically grown roots, during pre-symbiosis or during colonization by *P. microcarpus*; $n = 4$, ppb, parts per billion, ±SE. (c) Fold change in the concentration of ABA in *P. microcarpus* extra-radical mycelium in physical contact with *E. grandis* roots, as compared to axenically grown *P. microcarpus* mycelium, during pre-symbiosis or during colonization by *P. microcarpus*; $n = 3$, ppb, parts per billion, ±SE. (d) Heatmap to show the relative expression of *E. grandis* genes orthologous to *Arabidopsis thaliana* genes known to be positively regulated by ABA during *P. microcarpus* colonization. (e) Heatmap to show the relative expression of *E. grandis* genes orthologous to *A. thaliana* genes known to be negatively regulated by abscisic acid during *P. microcarpus* colonization.

Table 3 The majority of tested carotenoids in *Eucalyptus grandis* roots are significantly reduced during pre-symbiosis with *Pisolithus microcarpus*.

	Carotenoid content (μg g^{-1} fresh weight)						
Treatment	Neo	Vio	Ant	Lut	Zea	β-Car	Total
Control	1.011 (±0.095)	1.226 (±0.130)	0.473 (±0.070)	1.512 (±0.263)	0.182 (±0.028)	0.589 (±0.087)	4.993 (±0.648)
Pre-symbiosis	0.768 (±0.036)	0.914 (±0.090)	0.297 (±0.015)	0.883 (±0.058)	0.083 (±0.005)	0.422 (±0.022)	3.368 (±0.155)
P-Value	0.010	0.065	0.004	0.006	0.001	0.024	0.005

Quantified carotenoids after 48 h of pre-symbiotic setup include Neo (neoxanthin), Vio (violaxanthin), Ant (antheraxanthin), Lut (lutein), Zea (zeaxanthin), β-Car (β-carotene); ±SE. Significant differences between control (i.e. axenically grown) roots and pre-symbiotic roots was determined (Student's *t*-test; $n = 4$ biological replicates).

Table 4 Abscisic acid concentration in *Eucalyptus grandis* roots undergoing colonization by *Pisolithus microcarpus* are significantly induced during fungal integration into the root.

	Axenic	Pre-symbiosis	24 h	48 h	1 wk
Root	0.021 (±0.006)	0.023 (±0.001)	1.097 (±0.318)	0.213 (±0.051)	0.511 (±0.178)
P-Value (root)		0.75	5.1×10^{-4}	2.4×10^{-4}	2.2×10^{-3}
EMM	0.003 (±0.001)	0.005 (±0.002)	0.003 (±0.000)	0.001 (±0.001)	0.002 (±0.001)
P-Value (EMM)		0.45	0.72	0.19	0.27

Quantification of ABA in roots and in extramatrical mycelium (EMM). Concentrations in parts per billion ±SE. Statistics are based on change from axenic control (Student's *t*-test; $n = 4$ for roots, $n = 3$ for EMM).

defence response genes, linked to various biotic and abiotic stimuli, were activated at different stages in the colonization process, much like previous reports (Duplessis *et al*., 2005; Le Quéré *et al*., 2005; Larsen *et al*., 2015; Plett *et al*., 2015b; Liao *et al*., 2016). Most prominent within our defence-related gene dataset were 163 significantly regulated LRR/PR proteins, a class highlighted by Liao *et al*. (2016) to also be differentially regulated in various *Pinus* species in response to colonization by members of the *Suillus* genus. Sebastiana *et al*. (2014) report that these defence-related DEGs might be involved with fungal species recognition. There were, also, a number of dirigent-like defence genes that were downregulated throughout the fungal integration stage; these genes are associated with cell-wall reinforcement and their repression may be required to enable growth of *P. microcarpus* into the root apoplastic space (Sebastiana *et al*., 2014; Li *et al*., 2017). In terms of the biosynthesis of metabolic products, using GO, we found that genes involved in the synthesis of phenylpropanoids, terpenoids, and flavonoids were also enriched within our transcriptional profiling of *E. grandis*. Similar gene classes have been found to be regulated in EcM interaction with *Populus*, *Pinus*, and aspen, although the direction and magnitude of how these pathways are impacted is not consistent (Weiss *et al*., 1997; Li *et al*., 2014; Liao *et al*., 2014; Plett *et al*., 2015b; Basso *et al*., 2019). Transcriptomically Weiss *et al*. (1997), and metabolomically Plett *et al*. (2021a), found that phenylpropanoid and flavonoids were increased during the early stages of EcM colonization, compounds that Behr *et al*. (2020) were able to positively correlate with EcM colonization. In our results, however, we found these pathways were downregulated during the physical integration stage of colonization in *E. grandis* before being positively expressed during the functional symbiosis phase. Terpenoid associated genes, meanwhile, identified as being enriched during EcM colonization of host roots both here and by previous research (Behr *et al*., 2020) are known to be partially responsible

© 2021 The Authors
New Phytologist © 2021 New Phytologist Foundation. This article has been contributed to by US Government employees and their work is in the public domain in the USA.

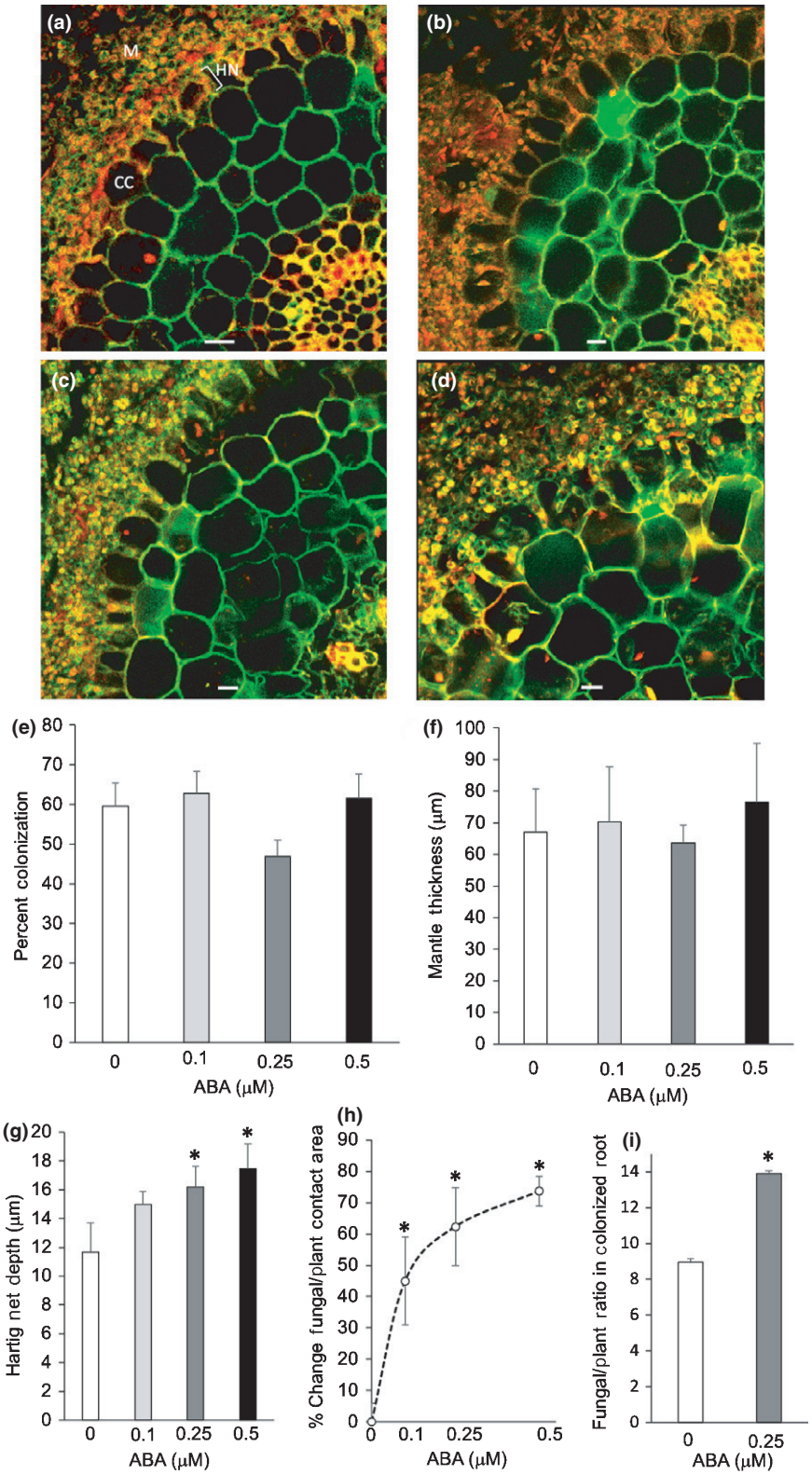

Fig. 5 Exogenous abscisic acid (ABA) enhances Hartig net development. (a) Representative image of a transverse cross-section of an *Eucalyptus grandis* lateral root colonized by *Pisolithus microcarpus* without the addition of ABA (M, mantle; HN, Hartig net; CC, cortical cell), with the addition of 0.1 μM ABA (b), 0.25 μM ABA (c), or 0.5 μM ABA (d); Bar, 10 μm in each image. (e) Percentage of total lateral roots in contact with *P. microcarpus* that were colonized under each concentration of exogenous ABA. No significant difference was found (Student's *t*-test; ±SE; $n = 6$). (f) Average mantle thickness across each treatment. No significant difference was found (Student's *t*-test; ±SE; $n = 6$). (g) Average Hartig net depth across each treatment; asterisk (*), significant difference from 0 μM ABA (Student's *t*-test; ±SE, $n = 6$). (h) Average percentage change in fungal/plant contact area, defined as the surface area of plant cells in primary contact with fungal hyphae normalized to root diameter, between 0 μM ABA and the addition of a given quantity of ABA; asterisk (*), significant difference from 0 mM ABA ($P < 0.05$); ±SE, $n = 6$. (i) Average fungal : plant ratio in excised mycorrhizal root tips. The ratio was calculated based on the transcript copy number of two fungal control genes normalized by the transcript copy number of a plant control gene between with either 0 or 0.25 μM ABA treated root systems; asterisk (*), significant difference from 0 mM ABA ($P < 0.05$); ±SE, $n = 4$.

for differentiation between different stages of the colonization process (Liao *et al.*, 2014; Basso *et al.*, 2019).

Terpenoids encompass a wide array of secondary metabolites including volatile signalling molecules, and carotenoids, and provide precursors for phytohormone biosynthesis (Huang & Osbourn, 2019). The comparative lack of information regarding the roles of carotenoids during EcM colonization, combined with the prominence of these pathways within our investigation, led us to focus on understanding their roles during EcM symbiosis. While these metabolites play a significant role in supporting AM

© 2021 The Authors
New Phytologist © 2021 New Phytologist Foundation. This article has been contributed to by US Government employees and their work is in the public domain in the USA.

14698137, 2022, 2, Downloaded from https://nph.onlinelibrary.wiley.com/doi/10.1111/nph.17825 by Inrae - Dipso, Wiley Online Library on [24/02/2023]. See the Terms and Conditions (https://onlinelibrary.wiley.com/terms-and-conditions) on Wiley Online Library for rules of use; OA articles are governed by the applicable Creative Commons License

14698137, 2022, 2, Downloaded from https://nph.onlinelibrary.wiley.com/doi/10.1111/nph.17825 by Inrae - Dipso, Wiley Online Library on [24/02/2023]. See the Terms and Conditions (https://onlinelibrary.wiley.com/terms-and-conditions) on Wiley Online Library for rules of use; OA articles are governed by the applicable Creative Commons License

root colonization (Welling *et al.*, 2016; Felemban *et al.*, 2019), their role in EcM systems has largely been investigated in the shoots of colonized hosts (Sebastiana *et al.*, 2013; Welling *et al.*, 2016). Within roots, AM fungal colonization leads to changes in lutein, lycopene, β-carotene and zeaxanthin (Welling *et al.*, 2016). While we observed reduced carotenoid levels in *E. grandis* roots during pre-symbiosis, we found that the transcription of genes enzymes leading to the synthesis of lycopene, β-carotene and zeaxanthin were induced while the genes related to lutein synthesis were repressed. Following on from β-carotene, the observed higher expression of *ZEAXANTHIN EPOXIDASE* and *9-CIS-EPOXYCAROTENOID DIOXYGENASE* could reveal a higher biosynthetic flow away from β-carotene and zeaxanthin, the preferred substrates required for the biosynthesis of the apocarotenoids stigolactones and zaxinone that promote AM symbiosis (Felemban *et al.*, 2019; Ablazov *et al.*, 2020). Our results would suggest that the biosynthetic flux of pre-existing intermediates was funnelled instead toward the production of ABA. In future it would be interesting to study if these alterations in carotenoid metabolic flux could further favour EcM colonization at the expense of competing AM fungi in dual host plants.

The plant hormone ABA is another product of the carotenoid pathway that our transcriptomic results would suggest is altered during EcM integration. ABA is known to have influence over various aspects of plant development and cellular metabolism, including mycorrhizal associations. There are a number of possible mechanisms by which ABA may be fostering beneficial plant–microbe interactions. In AM symbioses, ABA in low doses has been shown to support colonization through the signalling PROTEIN PHOSPHATASE 2A while higher levels of ABA negatively impact colonization through an inhibition of mycorrhizal induced host calcium oscillations (Charpentier *et al.*, 2014). ABA also interacts with other plant hormones, and its inhibition of ethylene signalling has been proposed as another pathway by which AM colonization is promoted (Herrera-Medina *et al.*, 2007; Martín-Rodríguez *et al.*, 2011). ABA may also influence colonization of AM fungi through the stimulation of antioxidant pathways (Lou *et al.*, 2021). Reports of the accumulation of, and signalling due to, ABA during EcM symbiosis are conflicting. Some studies found that there was no change to ABA concentration in EcM host roots (Coleman *et al.*, 1990; Calvo-Polanco *et al.*, 2019; Lou *et al.*, 2021), while another, like ours, found significant increases (Luo *et al.*, 2009). Certain reports have not found ABA signalling genes to be induced during EcM symbiosis (Rincón *et al.*, 2005), possibly due to only considering a select number of ABA-responsive genes, while other studies found that an additional stress is required before ABA signalling was affected (Luo *et al.*, 2009). In our system, we found that ABA concentration increased during the initial stages of fungal integration into the root. As a commensurate increase in ABA was not observed in the extraradical mycelium, and as the concentration of ABA in the mycelium was found to be orders of magnitude lower than in the colonized roots, this would suggest that the site of synthesis is in the plant cells. This was supported by the repression of *PSY* (which is negatively regulated by elevated ABA concentrations; Welsch *et al.*, 2008), by the upregulation of *E. grandis* genes in the majority of the biosynthetic pathway previous to ABA production, and by the expression of ABA responsive genes in the host root cell. Of note, we found that the differential expression of ABA-responsive genes was not uniform: only certain genes were induced/repressed as would be anticipated by elevated ABA concentrations. The mechanism by which this selectivity may occur is unknown, although as *Pisolithus* encodes effector-like proteins (Kohler *et al.*, 2015; Plett *et al.*, 2020) it may have the capability of targeting specific components of host hormone signalling pathways to effect this pattern of differential gene transcription. Our results with exogenous application of ABA also support the hypothesis that the hormone is involved in the control of *P. microcarpus* integration into the root during the Hartig net formation. This is similar to the proposed role of ABA in supporting AM fungal colonization of host roots by Zhang *et al.* (2019), highlighting a function that may be conserved across the evolution of mutualistic plants–fungal interactions.

Based on this study, we conclude that the colonization of *E. grandis* by an EcM partner significantly changes the regulation of a large portion of the host gene repertoire, particularly the carotenoid pathway and its derivative ABA metabolic signalling pathway. Future research should be undertaken to understand the triggers, consequences, and regulation of carotenoid derived apocarotenoids, as well as the role of ABA during mutualistic EcM associations in both *in vitro* and more natural soil-based systems. This would give us a more holistic understanding concerning the roles of carotenoids and hormones during both EcM and AM plant–microbe interactions.

Acknowledgements

The authors thank M Mikhael and D Wojtalewicz at the Western Sydney University Mass Spectrometry facilities for assistance with the carotenoid and hormone analyses, and the Western Sydney University Confocal Bio-Imaging Facility for access to its instrumentation. This research was funded by the Australian Research Council for a Discovery grant to ICA, JMP and FM (DP160102684) and the US Department of Energy Joint Genome Institute (CSP1953). This research was also supported by the Laboratory of Excellence ARBRE (ANR-11-LABX-0002-01) and the Plant–Microbe Interfaces Scientific Focus Area in the Genomic Science Programme, the Office of Biological and Environmental Research in the US Department of Energy (DOE) Office of Science. The work conducted by the US Department of Energy Joint Genome Institute, a DOE Office of Science User Facility, is supported by the Office of Science of the US DOE under contract no. DE-AC02-05CH11231.

Author contributions

RAH, JMP, KLP, JW-B, ICA, FM and TJ designed research. MW, AL, VN, IVG performed RNA-sequencing and RAH, JMP, KLP and TJ performed the analysis. RAH, DC, SA, CIC performed the carotenoid and hormone analyses. RAH, KLP, TJ,

© 2021 The Authors
New Phytologist © 2021 New Phytologist Foundation. This article has been contributed to by US Government employees and their work is in the public domain in the USA.

CIC and JMP wrote the article. All authors discussed the results and edited the manuscript.

ORCID

Ian C. Anderson https://orcid.org/0000-0002-3507-163X
Sidra Anwar https://orcid.org/0000-0002-0500-1649
Christopher I. Cazzonelli https://orcid.org/0000-0003-3096-3193
Donovin Coles https://orcid.org/0000-0003-3824-1881
Igor V. Grigoriev https://orcid.org/0000-0002-3136-8903
Richard A. Hill https://orcid.org/0000-0002-2678-796X
Francis Martin https://orcid.org/0000-0002-4737-3715
Vivian Ng https://orcid.org/0000-0001-8941-6931
Jonathan M. Plett https://orcid.org/0000-0003-0514-8146
Krista L. Plett https://orcid.org/0000-0001-6422-3754
Mei Wang https://orcid.org/0000-0002-3240-7994
Johanna Wong-Bajracharya https://orcid.org/0000-0001-6119-8645

Data availability

The data that supports the findings of this study are openly available in the National Centre for Biotechnology Information (NCBI) Short Read Archive at https://www.ncbi.nlm.nih.gov/sra, reference numbers SRX5064672-SRX5064689.

References

Ablazov A, Mi J, Jamil M, Jia K-P, Wang JY, Feng Q, Al-Babili S. 2020. The apocarotenoid zaxinone is a positive regulator of strigolactone and abscisic acid biosynthesis in *Arabidopsis* roots. *Frontiers in Plant Science* **11**: 578.

Akiyama K, Matsuzaki K, Hayashi H. 2005. Plant sesquiterpenes induce hyphal branching in arbuscular mycorrhizal fungi. *Nature* **435**: 824–827.

Alagoz Y, Dhami N, Mitchell C, Cazzonelli CI. 2020. *Cis*/trans carotenoid extraction, purification, detection, quantification, and profiling in plant tissues. In: Rodríguez-Concepción M, Welsch R, eds. *Plant and food carotenoids. Methods in molecular biology, vol. 2083*. New York, NY, USA: Humana, 145–163.

Alvarez M, Huygens D, Fernandez C, Gacitua Y, Olivares E, Saavedra I, Alberdi M, Valenzuela E. 2009. Effect of ectomycorrhizal colonization and drought on reactive oxygen species metabolism of *Nothofagus dombeyi* roots. *Tree Physiology* **29**: 1047–1057.

Amir Hossain M, Lee Y, Cho J-I, Ahn C-H, Lee S-K, Jeon J-S, Kang H, Lee C-H, An G, Park PB. 2010. The bZIP transcription factor OsABF1 is an ABA responsive element binding factor that enhances abiotic stress signaling in rice. *Plant Molecular Biology* **72**: 557–566.

Balestrini R, Bonfante P. 2014. Cell wall remodeling in mycorrhizal symbiosis: a way towards biotrophism. *Frontiers in Plant Science* **5**: 237.

Basso V, Kohler A, Miyauchi S, Singan V, Guinet F, Šimura J, Novák O, Barry KW, Amirebrahimi M, Block J *et al.* 2019. An ectomycorrhizal fungus alters sensitivity to jasmonate, salicylate, gibberellin, and ethylene in host roots. *Plant, Cell & Environment* **43**: 1047–1068.

Becquer A, Guerrero-Galán C, Eibensteiner JL, Houdinet G, Bücking H, Zimmermann SD, Garcia K. 2019. The ectomycorrhizal contribution to tree nutrition. *Advances in Botanical Research* **89**: 77–126.

Behr M, Baldacci-Cresp F, Kohler A, Morreel K, Goeminne G, Van Acker R, Veneault-Fourrey C, Mol A, Pilate G, Boerjan W *et al.* 2020. Alterations in the phenylpropanoid pathway affect poplar ability for ectomycorrhizal colonisation and susceptibility to root-knot nematodes. *Mycorrhiza* **30**: 555–566.

Besserer A, Puech-Pagès V, Kiefer P, Gomez-Roldan V, Jauneau A, Roy S, Portais JC, Roux C, Bécard G, Séjalon-Delmas N. 2006. Strigolactones stimulate arbuscular mycorrhizal fungi by activating mitochondria. *PLoS Biology* **4**: e226.

Bouffaud M-L, Herrmann S, Tarkka MT, Bönn M, Feldhahn L, Buscot F. 2020. Oak displays common local but specific distant gene regulation responses to different mycorrhizal fungi. *BMC Genomics* **21**: 399.

Brundrett MC, Tedersoo L. 2018. Evolutionary history of mycorrhizal symbioses and global host plant diversity. *New Phytologist* **220**: 1108–1115.

Calvo-Polanco M, Armada E, Zamarreño AM, García-Mina JM, Aroca R. 2019. Local root ABA/cytokinin status and aquaporins regulate poplar responses to mild drought stress independently of the ectomycorrhizal fungus *Laccaria bicolor*. *Journal of Experimental Botany* **70**: 6437–6446.

Cazzonelli CI, Hou X, Alagoz Y, Rivers J, Dhami N, Lee J, Marri S, Pogson BJ. 2020. A *cis*-carotene derived apocarotenoid regulates etioplast and chloroplast development. *eLife* **9**: e45310.

Charpentier M, Sun J, Wen J, Mysore KS, Oldroyd GE. 2014. Abscisic acid promotion of arbuscular mycorrhizal colonization requires a component of the PROTEIN PHOSPHATASE 2A complex. *Plant Physiology* **166**: 2077–2090.

Coleman MD, Bledsoe CS, Smit BA. 1990. Root hydraulic conductivity and xylem sap levels of zeatin riboside and abscisic acid in ectomycorrhizal Douglas fir seedlings. *New Phytologist* **115**: 275–284.

Cope KR, Bascaules A, Irving TB, Venkateshwaran M, Maeda J, Garcia K, Rush TA, Ma C, Labbé J, Jawdy S *et al.* 2019. The ectomycorrhizal fungus *Laccaria bicolor* produces lipochitooligosaccharides and uses the common symbiosis pathway to colonize *Populus* roots. *Plant Cell* **31**: 2386–2410.

da Silva CI, de Queiroz MV, Costa MD, Kasuya MCM, de Araújo EF. 2010. Identification of differentially expressed genes of the fungus *Hydnangium* sp. during the pre-symbiotic phase of the ectomycorrhizal association with *Eucalyptus grandis*. *Mycorrhiza* **20**: 531–540.

Ditengou FA, Muller A, Rosenkranz M, Felten J, Lasok H, van Doorn MM, Legue V, Palme K, Schnitzler JP, Polle A. 2015. Volatile signalling by sesquiterpenes from ectomycorrhizal fungi reprogrammes root architecture. *Nature Communications* **6**: 6279.

Duplessis S, Courty PE, Tagu D, Martin F. 2005. Transcript patterns associated with ectomycorrhiza development in *Eucalyptus globulus* and *Pisolithus microcarpus*. *New Phytologist* **165**: 599–611.

Felemban A, Braguy J, Zurbriggen MD, Al-Babili S. 2019. Apocarotenoids involved in plant development and stress response. *Frontiers in Plant Science* **10**: 1168.

Felten J, Kohler A, Morin E, Bhalerao RP, Palme K, Martin F, Ditengou FA, Legué V. 2009. The ectomycorrhizal fungus *Laccaria bicolor* stimulates lateral root formation in poplar and *Arabidopsis* through auxin transport and signaling. *Plant Physiology* **151**: 1991–2005.

Finkelstein R. 2013. Abscisic acid synthesis and response. *The Arabidopsis book* **11**: e0166.

Fiorilli V, Wang JY, Bonfante P, Lanfranco L, Al-Babili S. 2019. Apocarotenoids: old and new mediators of the arbuscular mycorrhizal symbiosis. *Frontiers in Plant Science* **10**: 1186.

Garcia K, Delaux P-M, Cope KR, Ané J-M. 2015. Molecular signals required for the establishment and maintenance of ectomycorrhizal symbioses. *New Phytologist* **208**: 79–87.

Hall CR, Waterman JM, Vandegeer RK, Hartley SE, Johnson SN. 2019. The role of silicon in antiherbivore phytohormonal signalling. *Frontiers in Plant Science* **10**: 1132.

Hamilton CE, Bauerle TL. 2012. A new currency for mutualism? Fungal endophytes alter antioxidant activity in hosts responding to drought. *Fungal Diversity* **54**: 39–49.

Herrera-Medina MJ, Steinkellner S, Vierheilig H, Ocampo Bote JA, García Garrido JM. 2007. Abscisic acid determines arbuscule development and functionality in the tomato arbuscular mycorrhiza. *New Phytologist* **175**: 554–564.

© 2021 The Authors
New Phytologist © 2021 New Phytologist Foundation. This article has been contributed to by US Government employees and their work is in the public domain in the USA.

14698137, 2022, 2, Downloaded from https://nph.onlinelibrary.wiley.com/doi/10.1111/nph.17825 by Inrae - Dipso, Wiley Online Library on [24/02/2023]. See the Terms and Conditions (https://onlinelibrary.wiley.com/terms-and-conditions) on Wiley Online Library for rules of use; OA articles are governed by the applicable Creative Commons License

Hogekamp C, Küster H. 2013. A roadmap of cell-type specific gene expression during sequential stages of the arbuscular mycorrhiza symbiosis. *BMC Genomics* **14**: 306.

Hortal S, Plett KL, Plett JM, Cresswell T, Johansen M, Pendall E, Anderson IC. 2017. Role of plant-fungal nutrient trading and host control in determining the competitive success of ectomycorrhizal fungi. *ISME Journal* **11**: 2666–2676.

Huang AC, Osbourn A. 2019. Plant terpenes that mediate below-ground interactions: prospects for bioengineering terpenoids for plant protection. *Pest Management Science* **75**: 2368–2377.

Jia K-P, Baz L, Al-Babili S. 2017. From carotenoids to strigolactones. *Journal of Experimental Botany* **69**: 2189–2204.

Kanehisa M, Furumichi M, Tanabe M, Sato Y, Morishima K. 2017. KEGG: new perspectives on genomes, pathways, diseases and drugs. *Nucleic Acids Research* **45**: D353–d361.

Kanehisa M, Goto S. 2000. KEGG: Kyoto Encyclopedia of Genes and Genomes. *Nucleic Acids Research* **28**: 27–30.

Kanehisa M, Sato Y, Furumichi M, Morishima K, Tanabe M. 2019. New approach for understanding genome variations in KEGG. *Nucleic Acids Research* **47**: D590–D595.

Kohler A, Kuo A, Nagy LG, Morin E, Barry KW, Buscot F, Canbäck B, Choi C, Cichocki N, Clum A *et al.* 2015. Convergent losses of decay mechanisms and rapid turnover of symbiosis genes in mycorrhizal mutualists. *Nature Genetics* **47**: 410–415.

Kulik A, Wawer I, Krzywińska E, Bucholc M, Dobrowolska G. 2011. SnRK2 protein kinases—key regulators of plant response to abiotic stresses. *OMICS: A Journal of Integrative Biology* **15**: 859–872.

Larsen PE, Sreedasyam A, Trivedi G, Desai S, Dai Y, Cseke LJ, Collart FR. 2015. Multi-omics approach identifies molecular mechanisms of plant–fungus mycorrhizal interaction. *Frontiers in Plant Science* **6**: 1061.

Le Quéré A, Wright DP, Söderström B, Tunlid A, Johansson T. 2005. Global patterns of gene regulation associated with the development of ectomycorrhiza between birch (*Betula pendula* Roth.) and *Paxillus involutus* (Batsch) Fr. *Molecular Plant–Microbe Interactions* **18**: 659–673.

Li H, Peng H, Wang L, Wei H, Li N, Jing Q. 2014. Identification of fungal genes involved in the preinfection events between ectomycorrhizal association (*Pisolithus tinctorius* and *Pinus massoniana*). *Mycological Progress* **13**: 123–130.

Li N, Zhao M, Liu T, Dong L, Cheng Q, Wu J, Wang LE, Chen XI, Zhang C, Lu W *et al.* 2017. A novel soybean dirigent gene GmDIR22 contributes to promotion of lignan biosynthesis and enhances resistance to *Phytophthora sojae*. *Frontiers in Plant Science* **8**: 1185.

Liao H-L, Chen Y, Bruns TD, Peay KG, Taylor JW, Branco S, Talbot JM, Vilgalys R. 2014. Metatranscriptomic analysis of ectomycorrhizal roots reveals genes associated with *Piloderma-Pinus* symbiosis: improved methodologies for assessing gene expression in situ. *Environmental Microbiology* **16**: 3730–3742.

Liao H-L, Chen Y, Vilgalys R. 2016. Metatranscriptomic study of common and host-specific patterns of gene expression between pines and their symbiotic ectomycorrhizal fungi in the genus *Suillus*. *PLoS Genetics* **12**: e1006348.

Lorente B, Zugasti I, Sánchez-Blanco MJ, Nicolás E, Ortuño MF. 2021. Effect of *Pisolithus tinctorious* on physiological and hormonal traits in *Cistus* plants to water deficit: relationships among water status, photosynthetic activity and plant quality. *Plants* **10**: 976.

Lou X, Zhang X, Zhang Y, Tang M. 2021. The synergy of arbuscular mycorrhizal fungi and exogenous abscisic acid benefits *Robinia pseudoacacia* L. growth through altering the distribution of Zn and endogenous abscisic acid. *Journal of Fungi* **7(8)**:671.

Love MI, Huber W, Anders S. 2014. Moderated estimation of fold change and dispersion for RNA-seq data with DESeq2. *Genome Biology* **15**: 550.

Luo Z-B, Janz D, Jiang X, Göbel C, Wildhagen H, Tan Y, Rennenberg H, Feussner I, Polle A. 2009. Upgrading root physiology for stress tolerance by ectomycorrhizas: insights from metabolite and transcriptional profiling into reprogramming for stress anticipation. *Plant Physiology* **151**: 1902–1917.

Maier W, Peipp H, Schmidt J, Wray V, Strack D. 1995. Levels of a terpenoid glycoside (Blumenin) and cell wall-bound phenolics in some cereal mycorrhizas. *Plant Physiology* **109**: 465–470.

Martin F, Kohler A, Murat C, Veneault-Fourrey C, Hibbett DS. 2016. Unearthing the roots of ectomycorrhizal symbioses. *Nature Reviews Microbiology* **14**: 760–773.

Martín-Rodríguez JÁ, León-Morcillo R, Vierheilig H, Ocampo JA, Ludwig-Müller J, García-Garrido JM. 2011. Ethylene-dependent/ethylene-independent ABA regulation of tomato plants colonized by arbuscular mycorrhiza fungi. *New Phytologist* **190**: 193–205.

Menotta M, Amicucci A, Sisti D, Gioacchini AM, Stocchi V. 2004. Differential gene expression during pre-symbiotic interaction between *Tuber borchii* Vittad. and *Tilia americana* L. *Current Genetics* **46**: 158–165.

Menotta M, Gioacchini AM, Amicucci A, Buffalini M, Sisti D, Stocchi V. 2004. Headspace solid-phase microextraction with gas chromatography and mass spectrometry in the investigation of volatile organic compounds in an ectomycorrhizae synthesis system. *Rapid Communications in Mass Spectrometry* **18**: 206–210.

Myburg AA, Grattapaglia D, Tuskan GA, Hellsten U, Hayes RD, Grimwood J, Jenkins J, Lindquist E, Tice H, Bauer D *et al.* 2014. The genome of *Eucalyptus grandis*. *Nature* **510**: 356.

Plett JM, Khachane A, Ouassou M, Sundberg B, Kohler A, Martin F. 2014. Ethylene and jasmonic acid act as negative modulators during mutualistic symbiosis between *Laccaria bicolor* and *Populus* roots. *New Phytologist* **202**: 270–286.

Plett JM, Kohler A, Khachane A, Keniry K, Plett KL, Martin F, Anderson IC. 2015. The effect of elevated carbon dioxide on the interaction between *Eucalyptus grandis* and diverse isolates of *Pisolithus* sp. is associated with a complex shift in the root transcriptome. *New Phytologist* **206**: 1423–1436.

Plett JM, Tisserant E, Brun A, Morin E, Grigoriev IV, Kuo A, Martin F, Kohler A. 2015. The mutualist *Laccaria bicolor* expresses a core gene regulon during the colonization of diverse host plants and a variable regulon to counteract host-specific defenses. *Molecular Plant–Microbe Interactions* **28**: 261–273.

Plett KL, Buckley S, Plett JM, Anderson IC, Lundberg-Felten J, Jämtgård S. 2021a. Novel microdialysis technique reveals a dramatic shift in metabolite secretion during the early stages of the interaction between the ectomycorrhizal fungus *Pisolithus microcarpus* and its host *Eucalyptus grandis*. *Microorganisms* **9**: 1817.

Plett KL, Kohler A, Lebel T, Singan V, Bauer D, He G, Ng V, Grigoriev I, Martin F, Plett JM *et al.* 2021b. Intra-species genetic variability drives carbon metabolism and symbiotic host interactions in the ectomycorrhizal fungus *Pisolithus microcarpus*. *Environmental Microbiology* **23**: 2004–2020.

Plett KL, Singan VR, Wang M, Ng V, Grigoriev IV, Martin F, Plett JM, Anderson IC. 2020. Inorganic nitrogen availability alters *Eucalyptus grandis* receptivity to the ectomycorrhizal fungus *Pisolithus albus* but not symbiotic nitrogen transfer. *New Phytologist* **226**: 221–231.

Pornsiriwong W, Estavillo GM, Chan KX, Tee EE, Ganguly D, Crisp PA, Phua SY, Zhao C, Qiu J, Park J *et al.* 2017. A chloroplast retrograde signal, 3′-phosphoadenosine 5′-phosphate, acts as a secondary messenger in abscisic acid signaling in stomatal closure and germination. *eLife* **6**: e23361.

Raudvere U, Kolberg L, Kuzmin I, Arak T, Adler P, Peterson H, Vilo J. 2019. g:Profiler: a web server for functional enrichment analysis and conversions of gene lists (2019 update). *Nucleic Acids Research* **47**: W191–W198.

Rincón A, Priha O, Lelu-Walter M-A, Bonnet M, Sotta B, Le Tacon F. 2005. Shoot water status and ABA responses of transgenic hybrid larch *Larix kaempferi* × *L. decidua* to ectomycorrhizal fungi and osmotic stress. *Tree Physiology* **25**: 1101–1108.

Rush TA, Puech-Pagès V, Bascaules A, Jargeat P, Maillet F, Haouy A, Maës AQ, Carriel CC, Khokhani D, Keller-Pearson M *et al.* 2020. Lipo-chitooligosaccharides as regulatory signals of fungal growth and development. *Nature Communications* **11**: 1–10.

Sandmann G. 2021. Diversity and origin of carotenoid biosynthesis: its history of co-evolution towards plant photosynthesis. *New Phytologist* **232**: 479–493.

Sebastiana M, Figueiredo A, Acioli B, Sousa L, Pessoa F, Baldé A, Pais MS. 2009. Identification of plant genes involved on the initial contact between ectomycorrhizal symbionts (*Castanea sativa* – European chestnut and *Pisolithus tinctorius*). *European Journal of Soil Biology* **45**: 275–282.

Sebastiana M, Pereira VT, Alcântara A, Pais MS, Silva AB. 2013. Ectomycorrhizal inoculation with *Pisolithus tinctorius* increases the performance

© 2021 The Authors
New Phytologist © 2021 New Phytologist Foundation. This article has been contributed to by US Government employees and their work is in the public domain in the USA.

14698137, 2022, 2, Downloaded from https://nph.onlinelibrary.wiley.com/doi/10.1111/nph.17825 by Inrae - Dipso, Wiley Online Library on [24/02/2023]. See the Terms and Conditions (https://onlinelibrary.wiley.com/terms-and-conditions) on Wiley Online Library for rules of use; OA articles are governed by the applicable Creative Commons License

of *Quercus suber* L. (cork oak) nursery and field seedlings. *New Forests* **44**: 937–949.

Sebastiana M, Vieira B, Lino-Neto T, Monteiro F, Figueiredo A, Sousa L, Pais MS, Tavares R, Paulo OS. 2014. Oak root response to ectomycorrhizal symbiosis establishment: RNA-Seq derived transcript identification and expression profiling. *PLoS ONE* **9**: e98376.

Seddas P, Gianinazzi-Pearson V, Schoefs B, Küster H, Wipf D. 2009. Communication and signaling in the plant–fungus symbiosis: the mycorrhiza. In: Baluka FE, ed. *Plant-environment interactions: from sensory plant biology to active plant behavior*. Berlin/Heidelberg, Germany: Springer, 45–71.

Splivallo R, Fischer U, Gobel C, Feussner I, Karlovsky P. 2009. Truffles regulate plant root morphogenesis via the production of auxin and ethylene. *Plant Physiology* **150**: 2018–2029.

Stauder R, Welsch R, Camagna M, Kohlen W, Balcke GU, Tissier A, Walter MH. 2018. Strigolactone levels in dicot roots are determined by an ancestral symbiosis-regulated clade of the PHYTOENE SYNTHASE gene family. *Frontiers in Plant Science* **9**: 255.

Tedersoo L, May TW, Smith ME. 2010. Ectomycorrhizal lifestyle in fungi: global diversity, distribution, and evolution of phylogenetic lineages. *Mycorrhiza* **20**: 217–263.

Tian F, Yang DC, Meng YQ, Jin J, Gao G. 2020. PlantRegMap: charting functional regulatory maps in plants. *Nucleic Acids Research* **48**: D1104–D1113.

Vivas M, Rolo V, Wingfield MJ, Slippers B. 2019. Maternal environment regulates morphological and physiological traits in *Eucalyptus grandis*. *Forest Ecology and Management* **432**: 631–636.

Weiss M, Mikolajewski S, Peipp H, Schmitt U, Schmidt J, Wray V, Strack D. 1997. Tissue-specific and development-dependent accumulation of phenylpropanoids in larch mycorrhizas. *Plant Physiology* **114**: 15–27.

Welling MT, Liu L, Rose TJ, Waters DLE, Benkendorff K. 2016. Arbuscular mycorrhizal fungi: effects on plant terpenoid accumulation. *Plant Biology* **18**: 552–562.

Welsch R, Wust F, Bar C, Al-Babili S, Beyer P. 2008. A third phytoene synthase is devoted to abiotic stress-induced abscisic acid formation in rice and defines functional diversification of phytoene synthase genes. *Plant Physiology* **147**: 367–380.

Willmann A, Thomfohrde S, Haensch R, Nehls U. 2014. The poplar NRT2 gene family of high affinity nitrate importers: impact of nitrogen nutrition and ectomycorrhiza formation. *Environmental and Experimental Botany* **108**: 79–88.

Wingfield MJ, Brockerhoff EG, Wingfield BD, Slippers B. 2015. Planted forest health: the need for a global strategy. *Science* **349**: 832–836.

Wong JWH, Lutz A, Natera S, Wang M, Ng V, Grigoriev I, Martin F, Roessner U, Anderson IC, Plett JM. 2019. The influence of contrasting microbial lifestyles on the pre-symbiotic metabolite responses of *Eucalyptus grandis* roots. *Frontiers in Ecology and Evolution* **7**: 10.

Zhang F, Wang P, Zou Y-N, Wu Q-S, Kuča K. 2019. Effects of mycorrhizal fungi on root-hair growth and hormone levels of taproot and lateral roots in trifoliate orange under drought stress. *Archives of Agronomy and Soil Science* **65**: 1316–1330.

Supporting Information

Additional Supporting Information may be found online in the Supporting Information section at the end of the article.

Fig. S1 Supporting control experiments to verify RNA-sequencing and influence of abscisic acid on medium pH.

Table S1 Primers used in the course of this study.

Table S2 The $\log_2$-fold change and statistical analysis of the 6687 *Eucalyptus grandis* differentially expressed genes (DEGs) during the colonization by *Pisolithus microcarpus*.

Table S3 List of the *Eucalyptus grandis* genes that most differentiate between colonization stages.

Table S4 *Eucalyptus grandis* genes whose expression most influences separation of the principal component analysis.

Table S5 Fold change in gene expression levels of carotenoid-associated biosynthetic enzymes during the colonization of *Eucalyptus grandis* by *Pisolithus microcarpus*.

Please note: Wiley Blackwell are not responsible for the content or functionality of any Supporting Information supplied by the authors. Any queries (other than missing material) should be directed to the *New Phytologist* Central Office.

About *New Phytologist*

- *New Phytologist* is an electronic (online-only) journal owned by the New Phytologist Foundation, a **not-for-profit organization** dedicated to the promotion of plant science, facilitating projects from symposia to free access for our Tansley reviews and Tansley insights.
- Regular papers, Letters, Viewpoints, Research reviews, Rapid reports and both Modelling/Theory and Methods papers are encouraged. We are committed to rapid processing, from online submission through to publication 'as ready' via *Early View* – our average time to decision is <26 days. There are **no page or colour charges** and a PDF version will be provided for each article.
- The journal is available online at Wiley Online Library. Visit **www.newphytologist.com** to search the articles and register for table of contents email alerts.
- If you have any questions, do get in touch with Central Office (np-centraloffice@lancaster.ac.uk) or, if it is more convenient, our USA Office (np-usaoffice@lancaster.ac.uk)
- For submission instructions, subscription and all the latest information visit **www.newphytologist.com**

© 2021 The Authors
New Phytologist © 2021 New Phytologist Foundation. This article has been contributed to by US Government employees and their work is in the public domain in the USA.

14698137, 2022, 2, Downloaded from https://nph.onlinelibrary.wiley.com/doi/10.1111/nph.17825 by Inrae - Dipso, Wiley Online Library on [24/02/2023]. See the Terms and Conditions (https://onlinelibrary.wiley.com/terms-and-conditions) on Wiley Online Library for rules of use; OA articles are governed by the applicable Creative Commons License